DIFFUSION AND ELASTOPLASTIC ANALYSES OF POLYCRYSTALLINE MAGNESIUM FOR SOLID STATE HYDROGEN STORAGE APPLICATION

by

AMEY MATHAKARI

Presented to the Faculty of the Graduate School of

The University of Texas at Arlington in Partial Fulfillment

of the Requirements

for the Degree of

MASTER OF SCIENCE IN MECHANICAL ENGINEERING

THE UNIVERSITY OF TEXAS AT ARLINGTON

DECEMBER 2015

To my dear father and mother for

their help and support throughout my life

Acknowledgements

Firstly, I thank my supervising professor Dr. Bo Yang, for guiding me, challenging me and believing in me. His patience and timely guidance help me to complete this thesis. Also, his constant guidance and encouragement make me go through both my graduate and internship program. The opportunity to work with him has been a great learning experience. I am grateful to Dr. Kent Lawrence and Dr. B. P. Wang, for serving on my thesis committee. I have benefited a great deal from their graduate lectures.

I am thankful to the Timber 410 guys and Yang Zhou, I couldn't have completed this work without their help. I am immensely thankful to my family who have always been supportive and stood by my decisions. It is their love that has motivated me to push myself forward and not to limit myself within my comfortable zone.

October 19, 2015

Abstract

DIFFUSION AND ELASTOPLASTIC ANALYSES OF POLYCRYSTALLINE MAGNESIUM FOR SOLID STATE HYDROGEN STORAGE APPLICATION

Amey Mathakari, M.S

The University of Texas at Arlington, 2015

Supervising Professor: Bo Yang

Solid state hydrogen storage can be an effective way of storing hydrogen as an energy source for mobile applications. The advantage includes high energy density, low setup cost, safe operation, abundance of metal hydrides, low maintenance, etc. Magnesium is one of the potential metals for the application. However, sluggish desorption kinetics of magnesium requiring relatively high operation temperature has hindered its practical realization. In the present study, an attempt is made to analyze effects of grain boundary on diffusion and diffusion induced stresses in polycrystalline magnesium. Grain boundaries in nanostructured magnesium can undergo severe plastic deformations during the hydrogen insertion and desertion processes. Such boundaries are characterized by excess grain boundary energy, presence of long range elastic stresses and enhanced pathways for hydrogen transport. Finite element models have been developed for the analyses by realizing the different physical and chemical parameters of magnesium grains and grain boundaries. The study provides convincing evidence of the importance of the presence of grain boundaries. The results may help find ways to improve hydrogen charging/discharging efficiency by means of plastic deformations in grain boundaries while maintaining the overall structural integrity of host magnesium.

Table of Contents

List of Illustrations

List of Tables

Chapter 1

INTRODUCTION

In last one decade hydrogen has attracted worldwide interest as a practicable source of energy. As hydrogen is light in weight, readily available and green source of energy, it can be used as source of fuel in automobile application. It can reduce petroleum and natural gas dependency in highly populated countries like India and China. This has generated comprehensive investigation on the technologies involved and how it is being resolved the difficulty of storing of hydrogen. The most common storage system is high pressure gas cylinder. In automobile sector Nissan developed a 70 MPa high pressure gas cylinder to improve the driving range of hydrogen vehicle. Another way of hydrogen storage is in liquid form. Liquid hydrogen is stored in cryogenic tanks at ambient temperature. Due to low critical temperature of hydrogen (33K) this can only be stored in open system, because there is no liquid phase existing above the critical temperature. Hence, this limits the use of liquid hydrogen storage in practical application. Moreover, challenges with liquid hydrogen storage are liquefaction process and thermal insulation of tank confines its use. In addition to this, both high pressure gas cylinder and liquid hydrogen storage require large storage tanks, high setup cost and have safety issues as hydrogen is highly inflammable. These difficulties can be overcome by using solid state hydrogen storage. An advantage of using solid state hydrogen storage includes; compact area for storage, low set up cost, safe operation, abundance of metal hydrides, low maintenance etc.

1.1. Solid State Hydrogen Storage Overview

Hydrogen storage through physical adsorption has great advantages in mobile applications. Hydrogen storage can be possible using carbon materials (Carbon Nanotubes, Graphite Nano Fiber, Graphene etc.) by adsorption technique as well as using chemical compounds (Zeolites, Metal Hydrides) by absorption technique. In solid-state storage, hydrogen is bonded by either physical (Metal-organic frame work and carbon based materials) or chemical forces (Hydrides, Nitrides) [15]. Physical adsorption has higher efficiency and faster adsorption-desorption rate, whereas chemical adsorption results in the adsorption of large amounts of gas. In some cases, adsorb gas require high temperature to get release.

Some of solid-state materials which are in use or under research are discussed below:

1.1.1. Carbon Nanotubes (CNT)

Nanocarbon materials contain defective structure, which can be useful for storing hydrogen. A typical SEM micrograph of a CNT at 10000x magnification is illustrated in Fig. 1.1.1[14]

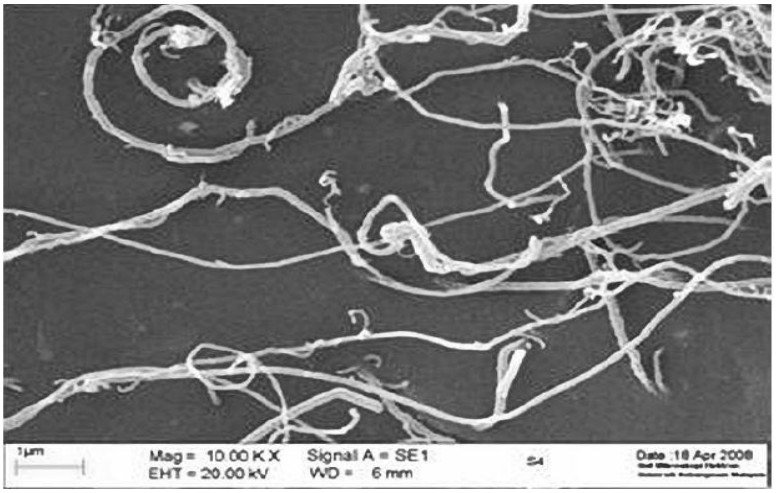

Figure 1.1 SEM micrograph of a CNT at 10000x magnification [14]

Dillon et al. [1], were first group found that the hydrogen storage capacity of CNTs, presented promising results. There are two main different species of CNTs; the single-walled nanotubes (SWNT) and the multi walled nanotubes (MWNT) [1]. As summarized in table1, very different hydrogen storage values between 0.25 and 56wt% have been reported in various experimental conditions. The storage capacity up to 6wt% is useful at cryogenic temperatures and with extremely high surface area carbons

Table 1.1 Summary of the reports of hydrogen storage capacity in carbon nanotubes.

Sample	T (K)	P (MPa)	H_2 (wt %)
SWNT	133	0.04	5–10
SWNT	A[a]	0.067	3.5–4.5
SWNT	77–300	8	1-15
SWNT	80	7	8.25
SWNT	A[a]	4.8	1.2
MWNT	298	12.16	56
MWNT	300–700	A[a]	0.25
MWNT	A	10	0.68
MWNT	300	1.0	13.8
MWNT	300	7.0	0.7–0.8

1.1.2. Graphite Nanofiber (GNF)

Graphite nanofibers (GFN) can be formed with chemical deposition method in which carbon containing gases are decomposed over a catalyst surface like metal or alloy and form carbon sheets. The carbon atoms precipitate at one or more surfaces forming continuous carbon sheets. This sheets stacks in one another to form GFNs. A schematic diagram of the GNF formation process is shown in Fig. 1.1.2. [1]

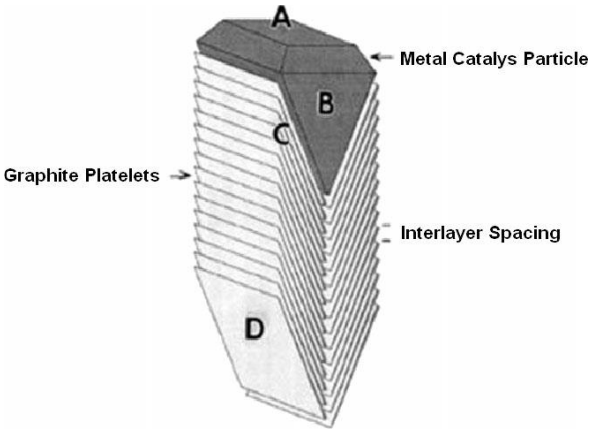

Figure 1.2 Scheme of GNF growth on a catalyst particle [1]

Researchers have produced graphite nanofibers at 500-600°C by passing ethylene (in an optimum ratio) with or without a carrier over some solid catalyst. It has been stated that the storage at room temperature and 12.16 MPa is 4.0 – 6.5 wt. %. But the mass production of nanomaterials with this method would be costly and very slow. [1] The best results were obtained from experiment done by Gupta et al [1]. Gupta et al [1] succeeded to grow GNF on gram scale per run by spray pyrolysis method involving benzene. The best measured result for hydrogen storage capacity on GNF was 10 wt. % at 27°C and 12.16 MPa.

1.1.3. Graphene

Graphene has enormous hydrogen storage density. Elias et al [1] have used a stream of hydrogen atoms to convert graphene reversibly in to graphene as shown in figure 1-1-3. The authors found that graphene can also release the stored hydrogen by heating at 450°C and the process is easy to implement. [15] According to Zhechkov et al. the graphene binding energy with most abundant atmospheric gas nitrogen is 18KJ.mol^{-1} [15]

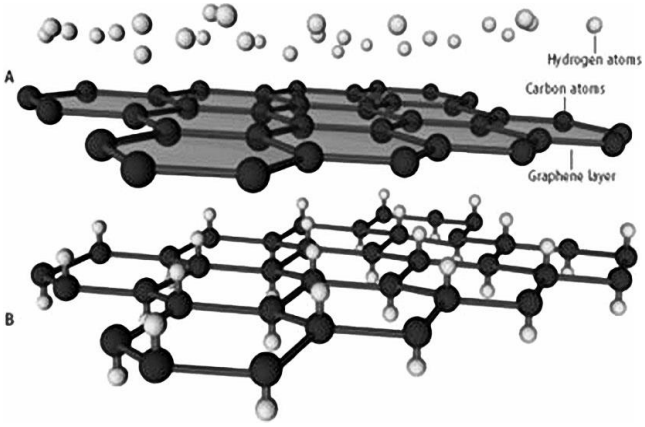

Figure 1.3 Hydrogen addition converting graphene (top) into graphane (bottom) [14]

Metal hydrides are very effective for storing large amount of hydrogen in very effective way. Metal compounds and alloys generally react with hydrogen and form mainly solid metal- hydrogen compound. Simple metal hydrides such as MgH2, transition metals as well as complex metal hydrides containing Li, Na, and Ca; for e.g. NaAlH4 and LaNi5H6 have been considered for this purpose. All these materials have good energy density by volume. Solid hydrides can be formed in pallets and granules. To release hydrogen content from these pallets requires temperature of 120°C. [2]

Detailed working of metal hydride storage system is discussed in following section. In most of the metal hydrides the hydrogenation and dehydrogenation process is carried out in same way. Magnesium hydride (MgH_2) is more convenient and cheaper to implement for solid state hydrogen storage. From table-1.1.4, we can get fair understanding that, for most practical applications, MgH_2 is a main candidate for research.

Table 1.2 Table-Volumetric and gravimetric hydrogen content in various materials. [1]

Material	H-atoms per cm^3 ($\times 10^{22}$)	Weight % hydrogen
H_2 gas, 200 bar (2850 psi)	0.99	100
H_2 liquid, 20 K (−253°C)	4.2	100
H_2 solid, 4.2 K (−269°C)	5.3	100
MgH_2	6.5	7.6
Mg_2NiH_4	5.9	3.6
$FeTiH_{1.95}$	6.0	1.89
$LaNi_5H_{6.7}$	5.5	1.37
$ZrMn_2H_{3.6}$	6.0	1.75
VH_2	11.4	2.10

1.2 Magnesium hydride for hydrogen storage

Magnesium has high hydrogen content 7.6 wt.% and also volumetric density is twice to that of liquid hydrogen. [12] Magnesium hydride has energy density i.e. 9MJ/kg Mg which is highest among all reversible hydride application for H-storage. [12] Magnesium hydride can store large quantity of Hydrogen than any other metal hydride. It is available in large quantities hence cheaper in cost.

McPhy has developed a unique technology for storing hydrogen in solid metal hydrides (MgH_2) at low pressure. This technology improves security related to hydrogen storage (compared to existing technologies: high pressure> 200 bar or liquid storage at -253 °C). There are two products of McPhy Energy based on solid state hydrogen storage used in industries since from 2011. The products are HES adiabatic storage and HDS non adiabatic having capacities of 24Kg and 100Kg of hydrogen respectively. Magnesium hydride composite situated at the central to the McPhy storage system is demonstrated in figure 1.2

Figure 1.4 McPhy composite (based on magnesium hydride)

Although there are many advantages of MgH_2 for storing hydrogen, some limitations need to overcome for its practical application. It includes, very slow hydrogenation and dehydrogenation reaction and this reaction occurs at high temperature 300-400K under a hydrogen pressure of more than 3MPa. This thesis mainly focuses on enhancement of hydrogenation and dehydrogenation process to get better hydrogen storage.

1.2.1 Magnesium Hydride formation

Formation of magnesium hydride is an exothermic reaction. The first study on the preparation of MgH_2 was given by Jolibois et al. [9] in 1912. In this study, MgH_2 was obtained by the pyrolysis of ethyl magnesium iodide in vacuum at 448K. The direct formation of this compound forming its element was reported after long time in 1951 by Wiberg et al [10]. But that was only 68% product. In 1984, Bogdanovic et al. [11] introduce two steps homogeneous catalysis. First step is transition of metallic magnesium to soluble form and second is the reaction of this solution with gaseous hydrogen in the presence of catalyst like $CrCl_3$, $TiCl_4$. But the process also has limitations as final product contains soluble impurity.

The complete process to get pure MgH_2 is mechano-chemical activation, in which, milling in a controlled atmosphere is used for the activation of solid phase reactions. This treatment creates activated outer surface along with mechanical defects and micro-strain crystal lattice. The mechano-chemical treatment of Mg in hydrogen atmosphere provides additional benefits such as hydrogenation of Mg at room temperature, easy diffusion in each layer of material due to mechanical action. [1]

Fundamentally, hydrogenation process can be divided in to three key steps [6]: Hydrogen dissociation, hydrogen diffusion and hydride formation. First step involves hydrogen dissociation on the metal surface of magnesium. Some catalyst can be introduced on the magnesium surface during this process to lower the operating temperature. This step is fairly simple to understand. In second step is more complicated as it involves many factors such as grain boundaries, vacancies, material formation (MgH_2), hydrogen pressure (Initial concentration of hydrogen) and grain boundaries modification. The third step in hydrogenation covers MgH_2 formation. This step is complex because of interaction of MgH_2 and hydrogen diffusion. It also includes morphology of MgH_2 along the Mg surface and along grain boundaries. Simple flow to understand hydrogenation steps is illustrated in figure 1.2.1

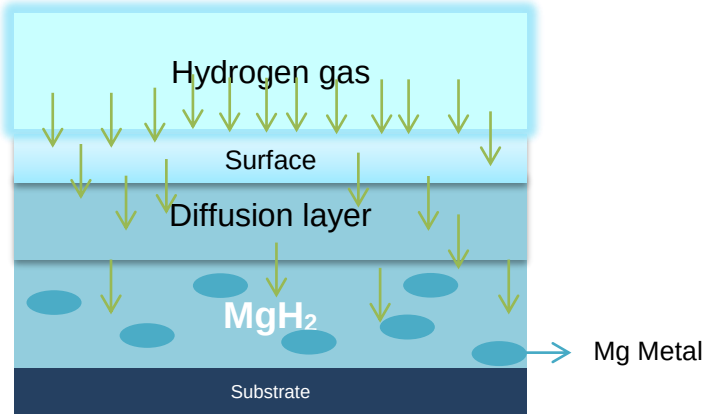

Figure 1.5 Different segments in MgH2 formation.

Additionally, there are several factors that significantly hindered the rate of hydrogenation for e.g. surface oxidation of magnesium when exposed to air is one of them. To initiate hydrogen absorption, the oxide layer should be broken down by activation process. In addition to this, consistent activation of hydrogen absorption requires cyclic heating and cooling in vacuum or in hydrogen atmosphere.

One more reason of the slow kinetics of hydrogenation is low dissociation rate of hydrogen molecules on the metal surface. Moreover, diffusion of hydrogen with in metal hydride is very difficult. Growth rate of magnesium hydride is also depends on hydrogen pressure. If the initial pressure is more, initial hydrogenation process gets fast as a result magnesium layer is formed on the surface which blocks hydrogen to penetrate further. [14] Hence, hydride phase occurs in slow-moving way resulting hydrogen diffusion only along the interface and not through hydride layer.

Mg-MgH_2 systems can be modified to improve the absorption/desorption characteristics. Following are the methods which can be applied to improve hydrogenation dehydrogenation process. [4]

1. Improving surface and kinetic properties by Ball Milling
2. Using Catalyst such as Ti, V, Ni and Fe.
3. Using thin film hydride and allowing other transition metal and their oxides.

All these techniques have given promising results, but the ball milling technique is most effective and common technique. Advantages of ball milling technique for desorption of hydrogen from magnesium hydride is described below.

By ball milling, the particle size gets reduced and surface roughness increases. The surface area increases from 1 to $10 m^2 g^{-1}$. Defects such as, increase in nucleation sites and a reduction in the diffusion path length for hydrogen leaving the hydride are introduced. This approach can reduce desorption time significantly. Additionally, it also overcome the

possibility of recombination of hydrogen atoms before desorption and diffusion pathway of hydrogen through magnesium grain structure[2]. The temperature for dehydrogenation by ball milling can be lowered up to 50^0C[2]. Ball milling of magnesium hydride also does internal defects (grain boundary) and internal stresses in structure.

1.2.2. Kinetics models of Hydrogen absorption/desorption

There are numbers of kinetic models available that explains the potential mechanism of hydrogen absorption and desorption from MgH_2. The equations for models are as follows: (Barkhordarian et al., Mintz and Zeiri et al.) [2]

SC1: $\alpha = kt$

JMA2: $[-\ln(1-\alpha)]^{1/2} = kt$ JMA3: $[-\ln(1-\alpha)]^{1/3} = kt$

CV2: $[-\ln(1-\alpha)]^{1/2} = kt$ CV3: $[-\ln(1-\alpha)]^{1/3} = kt$

CVD3: $1 - \frac{2\propto}{3} - (1-\alpha)^{2/3} = kt$

Where,

α – Transformed fraction

k – Reaction constant

t – Time

SC1 represents surface controlled reaction. Here, chemisorption of hydrogen is rate limiting step. JMA2 (2D) and JMA3 (3D) are Johnson-Mehl-Avrami models. These models represent nucleation and growth at random points in the bulk. In this model, rate limiting step is the constant velocity of moving interface between Mg and MgH_2. CV2 (2D) and CV3 (3D) represents for contracting volume models where, nucleation starts at the surface of sample. CVD3 is a model for hydrogen diffusion as a rate limiting step.

Magnesium hydride is a stoichiometric compound with atomic ratio of 0.99±0.01 (H/Mg). [2] In normal pressure condition, magnesium hydride (α-MgH_2) has tetragonal crystal structure. Figure 1.0032.2.shows magnesium and magnesium hydride (α-MgH_2)

crystal structure. Under high pressure α-MgH_2 undergoes polymorphic transformations [4] to form β- MgH_2 (orthorhombic structure) and Ɣ- MgH_2 (hexagonal structure).

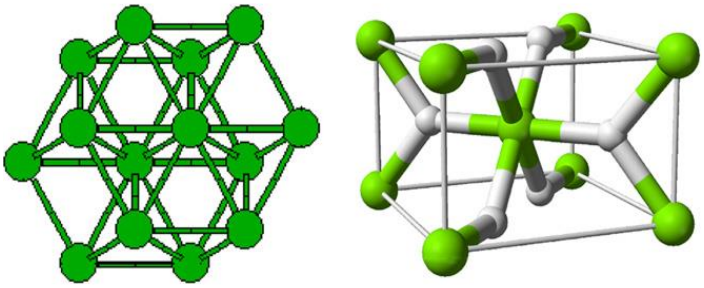

Figure 1.6 Crystal structure of Magnesium (Left) and Magnesium Hydride (α-MgH2)(Right) [5]

1.2.3. Grain Boundary Diffusion

As discussed earlier, diffusion of hydrogen atoms through magnesium crystal during absorption and desorption is an interesting phenomenon to increase efficiency of the overall process. It is second step in hydrogenation which involves many difficulties. Magnesium crystal is a hexagonal close pack structure. In which, hydrogen can occupy in either tetrahedral (T_d) holes or in octahedral (O_d) holes as shown in figure 1.2.3 (a) The hydrogen atom prefers to occupy T_d holes as the binding energy of T_d holes is -0.04eV, whereas binding energy of O_d holes is -0.21eV. [8] According to study of Finnabogi Oskarsson et al, William Stier et al, Hannes Johnsson et al. [8]; this is because octahedral hole is considerable larger than tetrahedral hole in Mg-H. Now the hydrogen atoms in T_d holes moves to other close T_d hole in two different ways: it can travel to the closest T_d hole which is normal to close pack plane or it can diffuse to non-neighboring T_d hole. As there is only one closest T_d hole, hydrogen atoms diffuse through the crystal initiating diffusion process in Mg grains. Similar mechanics is applied for diffusion of hydrogen through octahedral holes. Figure 1.2.3(b) shows the motion of hydrogen atoms through Mg- grains.

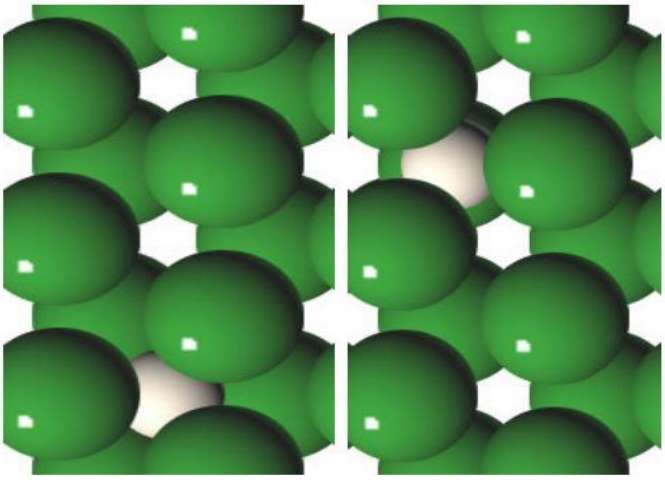

Figure 1.7 (a) Types of holes in Magnesium structure that hydrogen can occupy: Octahedral Holes (Left) and Tetrahedral Holes (Right) [8]

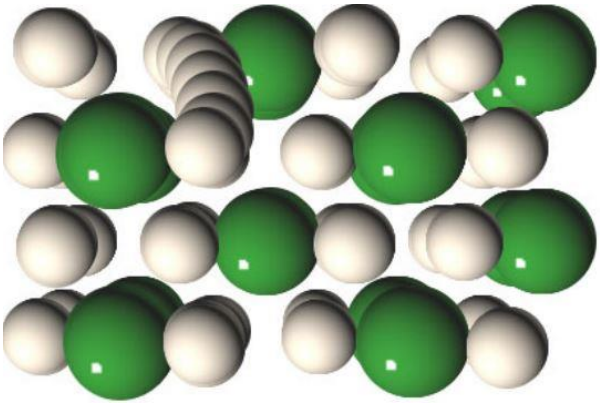

Figure 1.8 (b) Motion of Hydrogen atoms through grain boundary, and other hydrogen atom trapped in grain structure. [8]

In present thesis, the main focus is on the study of diffusion of hydrogen though grain boundaries and morphological changes formed during diffusion.

1.3. Motivation and Objectives

1.3.1. Motivation

Magnesium hydrides are capable of storing hydrogen at volume density that can replace compressed hydrogen gas and liquid hydrogen systems. Their weight efficiencies

reach 7.6 wt.% and their hydrogen desorption temperature are in the range of 100-400^{0}C at 1 bar hydrogen pressure. But, there are many challenges in the practical application of magnesium hydride for hydrogen storage. Understanding the importance of magnesium for hydrogen storage, researchers all over the world are involved in the study of Mg nano composites using various transition metal catalyst, thin films, multilayer films etc. Bo Yang et al, Yuping He et al., Yiping Zhao et al. [12] have studied hydrogen diffusion process of magnesium nanoblades coated with vanadium (V) as a catalyst. In this study hydrogen model is developed which separates hydrogen adsorption and interior diffusion during hydrogenation and dehydrogenation. Xiangwen Chen et al., Yuping Heet et al., Yiping Zhao et al. and XinweiWang et al. [13] studied thermophysical properties such as thermal conductivity and density of MgH_2 nanostructure. According to this study, thermal conductivity of hydrogenated MgH_2 is in range of 1.16-2.40 $Wm^{-1}K^{-1}$ and density is in range of 878-1320 Kg m^{-3}. Here oblique angle deposition technique is used to fabricate vanadium coated magnesium nanostructure and hydrogenated/dehydrogenated for 21 cycles. During hydrogenation/dehydrogenation coefficient of diffusion can be varied depending upon external factors. There are other factors such as nature of additive, cycling temperature, initial grain structure, which have significant impact on hydrogenation/dehydrogenation process. Therefore, study of grain boundary diffusion and morphological changes during hydrogenation/dehydrogenation could be effective to way to study magnesium hydride nanostructure more meticulously.

1.3.2. Objectives

The objectives are to examine the diffusion of hydrogen through grain boundaries of magnesium nanostructure. And, in what way the motion of hydrogen atoms through grain boundary affects the morphology of grain boundary and overall grain structure. Analogy between thermal diffusion and chemical diffusion is executed to perform chemical diffusion

analysis on the basis of Fick's first and second laws. Additionally, chemo stress analysis of grain boundary is carried out in this project with ANSYS simulation. This simulation study would provide insights in morphological changes in grain boundaries during hydrogen insertion with various material properties and geometries.

Chapter 2

PROBLEM FORMULATION

This chapter presents the theory of diffusion of hydrogen through magnesium crystalline grain and grain boundary. The constitutive governing equation for diffusion through isolated grain boundary model is built on the basis of mass transport phenomenon. Basically, mass transport is based on Fick's law of diffusion which is equivalent to Fourier's law of heat conduction. In later part of this work, Finite element model is defined for grain boundary structure which gives fair idea of diffusion process through the grain boundary and how morphological changes occurred in grain boundary due to flow of hydrogen atoms.

2.1. Problem Description

Grain boundaries between crystalline grains contain large amount of hydrogen that give rise to possible way for improved hydrogenation and dehydrogenation process. The heterogeneous nature of grain boundary from crystalline grain structure makes it interesting in physical properties as well as overall property of nano structure. This project studies overall diffusion pattern of hydrogen through grain boundaries. It also includes, chemo-stresses that are developed on grain boundaries during hydrogenation and dehydrogenation process. Figure 2.1.1 shows brief idea about the Mg grain – grain boundary structure and diffusion of hydrogen through it.

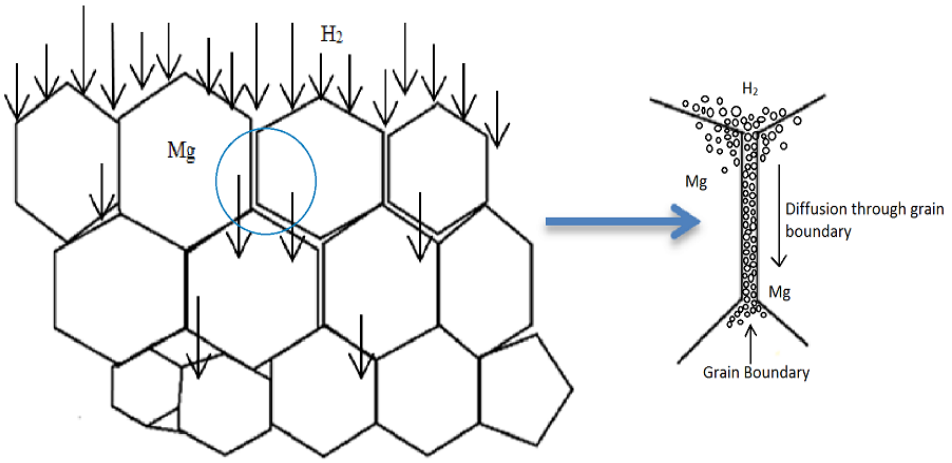

Figure 2.1 Diffusion of H¬2 through Mg nanostructure

To initiate with crystalline grain and grain boundary model, we have considered a single grain boundary between two crystalline grains as shown in figure 2.1.2. This gives exact idea about the overall magnesium crystalline nanostructure and our area of interest. We considered a single grain boundary to avoid complexities in modeling as shown in figure 2.1.2. Grain boundary is treated as a separate component which clutches two crystalline grains together. Governing equation for hydrogen diffusion through grain boundary is proposed in last part of this chapter.

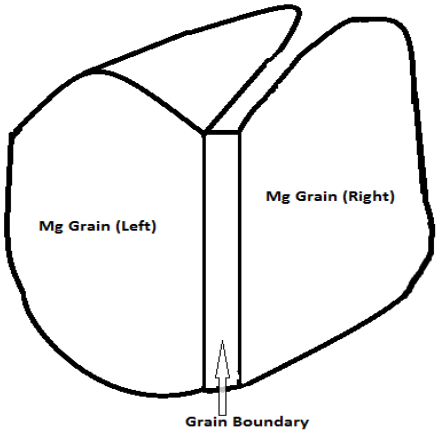

Figure 2.2 Single grain boundary between two Mg grains

When hydrogen atoms diffuse through the system, it is expected that, the rate of hydrogen atoms passing through the grain boundary will be more than that of crystalline grain structure and the size of grain boundary will also get increase significantly. And this leads to morphological changes in grain boundary structure which is studied in further part of this project.

2.2. Basic equations for mass transport

The diffusion of hydrogen in metals is based on Fick´s first laws of diffusion, with proper consideration of the geometry and boundary conditions of a given system. According to Fick's first law in one dimension, the diffusion flux goes from high concentration to region of low concentration with certain magnitude proportional to the concentration gradient. This can be stated in mathematical form as follow:

$$J = -D\frac{\partial C}{\partial x} \qquad (2.1)$$

Fick's first law can be easily generalized for 3-diamension case using vector notation as shown is equation (2.2). In isotropic material diffusivity is a scalar quantity. The vector J (diffusion flux) is in opposite direction to the concentration gradient vector, ∇C. Here nabla (∇) symbol represents vector operation and it acts on the scalar concentration field *C (x, y, z, t)* and produces concentration gradient field ∇C.

$$J = -\mathrm{D}\nabla C \qquad (2.2)$$

Units: The diffusion flux (*J*) is expressed as number of particles diffusing a unit area per unit time. Correspondingly, concentration (*C*) is number of particles per unit volume i.e. mol/vol. Diffusion coefficient (D) has unit depending on length and time of diffusion stated as, m^2/s.

In diffusion process number of diffusing particles is conserved. [*] To understand this let's consider an arbitrary system located at (x, y, z) and test volume is considered of size ∆x, ∆y, ∆z. as shown in figure2.2.1. The diffusion flux component entering the system is taken as Jx, Jy, Jz whereas, (Jx+ΔJx), (Jy+ΔJy), (Jz+ΔJz) are diffusion flux components coming out of the system. The physical equilibrium can be express as, Inflow – Outflow = Accumulation (Loss) Rate. This is simplified in equation (2.3).

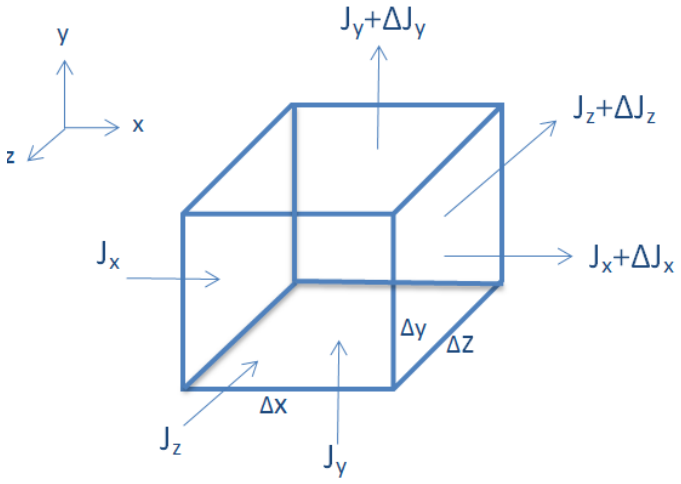

Figure 2.3 Flux components on magnesium grain

$$[Jx.\Delta y\ \Delta z\ \Delta t - (Jx + \Delta Jx).\Delta y\ \Delta z\ \Delta t] + [Jy.\Delta x\ \Delta z\ \Delta t - (Jy + \Delta Jy).\Delta x\ \Delta z\ \Delta t] +$$

$$[Jz.\Delta y\ \Delta x\ \Delta t - (Jz + \Delta Jz).\Delta y\ \Delta x\ \Delta t] = \Delta C.(\Delta x\ \Delta y\ \Delta z) \qquad (2.3)$$

By dividing equation (2.3) by total volume and time (ΔxΔyΔzΔt) and cancelling opposite terms, we get,

$$-\frac{\Delta Jx}{\Delta x} - \frac{\Delta Jy}{\Delta y} - \frac{\Delta Jz}{\Delta z} = \frac{\Delta C}{\Delta t} \qquad (2.4)$$

Taking limit as ∆ → 0 and solving equation (2.4) we get,

$$\frac{\partial C}{\partial t} = -\nabla \cdot \vec{J} \qquad (2.5)$$

Substituting *J* from equation 2 into above equation (2.5)

$$\frac{\partial C}{\partial t} = \nabla \cdot (\mathrm{D}\nabla C) \qquad (2.6)$$

This is Fick's second law of diffusion. For constant diffusion coefficient, it is linear second order partial differential equation. Equation for Cartesian co-ordinates (for Fick's second law equation) is given below:

$$\frac{\partial C}{\partial t} = \mathrm{D}\left(\frac{\partial^2 C}{\partial x^2} + \frac{\partial^2 C}{\partial y^2} + \frac{\partial^2 C}{\partial z^2}\right) \qquad (2.7)$$

At this point we can correlate Fick's law with Fourier law of heat conduction, where mass flux (kg/m^2s) is analogous with heat flux (W/m^2). Also, diffusion coefficient (m^2/s) and concentration (mol/vol.) are similar with thermal conductivity (W/mK) and temperature (K).

2.3. Mathematical formulation of grain boundary diffusion in isolated grain boundary model.

It is difficult to take real grain boundary structure to study on a continuum level. Here, we describe idealized model in which grain structure follows general Fick's second law of diffusion but this is not the case for grain boundary formulation. General description of diffusion along the grain boundary is outlined in figure 2.2.1. Structure of grain boundary in nanocrystalline material is similar to that of coarse grain size material. In this case free source (Hydrogen) is perpendicular to surface. Additionally, flow of hydrogen is continuous at the surface.

Consider figure 2.1.2, in which, two grains are separated by grain boundary and hydrogen is passing through it. Diffusion flux component passing through different directions is pictured in figure. 2.2.1. Let the size of grain boundary be '*h*' in x – direction. So, net flux entering and going out through the system is formulated in equation (2.8).

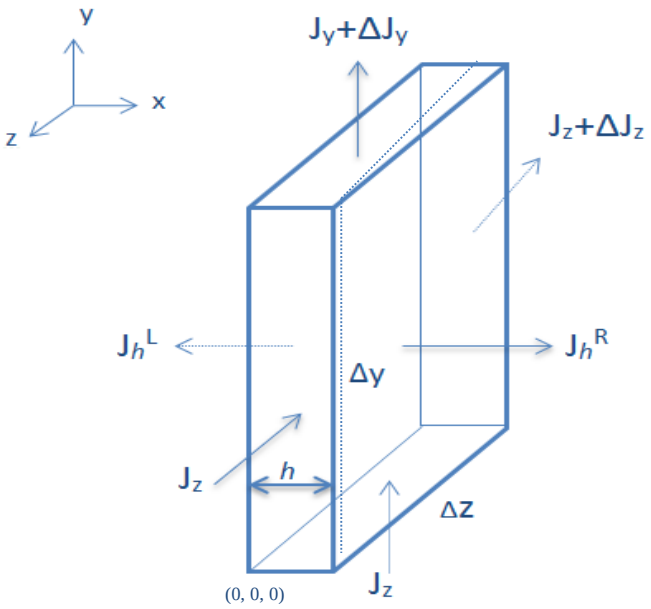

Figure 2.4 Flux components on grain boundary

The flux component can be written as,

$$[-Jh^{R}.\Delta y\,\Delta z\,\Delta t - Jh^{L}\Delta y\,\Delta z\,\Delta t] + [Jzh\,\Delta y\,\Delta t - (Jz + \Delta Jz)\Delta x\,\Delta z\,\Delta t] +$$

$$[Jy\,h\,\Delta z\,\Delta t - (Jy + \Delta Jy)h\,\Delta z\,\Delta t] = \Delta C\,(h\,\Delta y\,\Delta z\,) \qquad (2.8)$$

Where, Jh^{R} and Jh^{L} are diffusion fluxes on right and left side of grain boundary in *yz* – plane. And '*h'* is size of grain boundary in x – direction

Here, in this case, flux on grain boundary in *yz* – plane is taken as negative implying that the fluxes on both right and left sides of grain boundary gives diffusion flux in outward direction. As hydrogen concentration through grain boundaries are much more than that of hydrogen flowing through the grain in both right and left direction causing concentration difference. This causes diffusion flux to be in outer side in both cases i.e. on left and right side. Additionally, size of grain boundary is '*h*' in *yz* – plane and is considered as a constant throughout structure.

Now, divide all components by total volume and time gives following expression:

$$-\left(\frac{Jh^R+Jh^L}{h}\right)-\left(\frac{\Delta Jy}{\Delta y}+\frac{\Delta Jz}{\Delta z}\right)=\frac{\Delta C}{\Delta t} \qquad (2.9)$$

Taking limit as $\Delta \rightarrow 0$, we get,

$$\frac{\partial C}{\partial t}=-\nabla_s\cdot\vec{J}-\left(\frac{Jh^R+Jh^L}{h}\right) \qquad (2.10)$$

Applying Fick's first law and substituting *J* from equation (2.2), we get governing equation for grain boundary in isotropic, homogeneous and steady state condition.

$$\frac{\partial C}{\partial t}=-\nabla_s\cdot(-\mathrm{D}\nabla_s C)-\left(\frac{Jh^R+Jh^L}{h}\right) \qquad (2.11)$$

$$\frac{\partial C}{\partial t}=\mathrm{D}\nabla_s^2 C-\left(\frac{Jh^R+Jh^L}{h}\right) \qquad (2.12)$$

Where, in Cartesian co-ordinates,

$$\nabla_s^2=\left(\frac{\partial^2}{\partial y^2}+\frac{\partial^2}{\partial z^2}\right) \qquad (2.13)$$

Here, we separated overall model in to three parts (Grain to the left, grain to the right and grain boundary). But in real situation, grains are not detached from each other, as they are just separated by grain boundaries. So the continuity plays an important role while formulating this problem. As, hydrogen concentration in grain boundaries is much more than adjacent grain, there is possibility of flowing mass (hydrogen) from grain boundary to grain with certain flux. In present situation, Jh^R and Jh^L are outward fluxes from grain boundary to right and left side of gain respectively. The amount of flow of mass (hydrogen) depends on concentration of hydrogen on each side of grain. Also, amount of mass free from surface of grain boundary in particular side (right or left) at particular time is same as amount of mass gained by grain surface on respective side at the same time. In this way, the continuity gets satisfied on the grain and grain boundary interface. So the continuity equation can be written as,

$$Cg\,(x,y,t)=Cb\,(x,y,t) \qquad (2.14)$$

$$Jh^R(x,y,t)=Jg^R(x,y,t) \qquad \text{For } x=h/2 \qquad (2.15)$$

$$Jh^{L}(x,y,t) = Jg^{L}(x,y,t) \qquad \text{For x= - } h/2 \qquad (2.16)$$

Where J_g^L and J_g^R are diffusion flux of grain (left and right side respectively) on grain boundary side surface.

2.4. Chemical stress

This section introduced the theory of chemical stresses induced during hydrogenation/dehydrogenation process and what the ANSYS simulations are based on. In this project grain boundary undergoes large deformations during charging process due to insertion of hydrogen. This origins chemical stresses with in grain boundaries as well as in grain structure. Sometimes, the rate of hydrogen insertion is in such a large quantity that sets permanent deformations in grain boundaries. This arises chemical stresses in the system. It is always important to maintain structural integrity between grain and grain boundary to have better hydrogenation/ dehydrogenation rate. At the same time, if grain boundary bulges keeping all grains in connection improves overall efficiency of system. Therefore, we have consider chemical stress – strain relationship in this section and studied it with ANSYS considering different geometry and material property parameters.

The constitutive chemical stress equation shows a similar link with thermal stress equation. Hydrogen insertion (chemical expansion) causes grain and grain boundary to expand and contract. Consider, L is the original length of grain boundary and ΔL is change in length due to concentration change. Additionally, $\boldsymbol{\alpha}_b$ is chemical expansion coefficient for grain boundary. Now, the expansion is linearly proportional to change in concentration and ΔC is change in concentration. Therefore, deformation associated with it is given by,

$$\delta_c = \boldsymbol{\alpha}_b \, x \, \Delta C \qquad (2.17)$$

Figure 2.5 Chemical expansion in Grain boundary.

Now, the deformation is given by expansion divided by the original length through standard relation.

$$\delta c = \frac{\Delta L}{L} \qquad (2.18)$$

Where, δ_c – deformation in grain boundary due to chemical expansion

Hence, from equation (2.17) and (2.18), deformation due to concentration change is

$$\Delta L = \alpha c. L. \Delta C \qquad (2.19)$$

Now, deformation due to equivalent axial stress

$$\delta p = \frac{P.L}{A.E} \qquad (2.20)$$

Where, δ_p = deformation due to equivalent axial stress,

But, $\delta p = \delta c$

$$\alpha c. L. \Delta C = \frac{P.L}{A.E} \qquad (2.21)$$

$$\sigma = E.\alpha c.\Delta C \qquad (2.22)$$

Here, $\boldsymbol{\sigma}$ = Chemical stress, E = Young's Modulus.

Chapter 3

DIFFUSION ANALYSIS OF POLYCRYSTALLINE MAGNESIUM.

Diffusion phenomenon in magnesium grain and grain boundary can be further discussed with finite element analysis approach. Simple model is developed in ANSYS to demonstrate the concept regarding diffusion through grain boundary with considering different factors such as size of grain boundary, diffusion coefficient and diffusion time. In later part of this chapter multigrain polycrystalline model is developed to get overall understanding of the diffusion phenomenon.

3.1. Single crystal polycrystalline magnesium grain and grain boundary

3.1.1. Geometry

In realistic thousands of nanocrystalline grains are combined to form dense structure of magnesium to store hydrogen. Here, we are considering single crystal to understand diffusion patterns during hydrogenation and dehydrogenation. Figure 3.1.1 shows grain and grain boundary. Axisymmetric polycrystalline grain is developed and dimensions are normalized with magnesium grain, L, to avoid errors due to nano size complexities. Height of grain and grain boundary is given as H and length of grain boundary as L'. In actual scenario, size of magnesium grain is about 100nm while size of grain boundaries can be varied from 10-20nm.

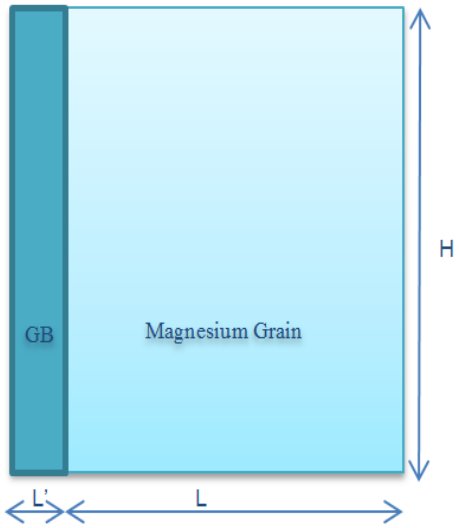

Figure 3.1 Geometry of Single Grain boundary attached to Mg Grain

Dimensions for simple polycrystalline structure are given as:

$$L = 1$$

$$L' = 0.1L$$

$$H = 1L$$

3.1.2. Material Properties

In this project, material properties are all define according to Fick's law of diffusion. It needs to be clarifying that this diffusion problem is mass transfer problem analogous with transient thermal conduction problem. However, the density and specific heat parameter does not play role in the simulation because basic governing equation for mass transport diffusion is given as: $\mathrm{m} = -D\nabla C$

Hence, input values for both density and specific heat are assumed to be unity. Now, the only parameter which plays role for diffusion process is chemical diffusivity. For magnesium nanocrystal grain and grain boundary different coefficient of diffusion can be subjected to manufacturing process and presence of catalyst. To get general understanding of system we have consider normalized diffusion coefficient of magnesium

polycrystalline grain as 1 and diffusion coefficient of grain boundary is parameterized to study different diffusion patterns for twist GB, tilt GB and twist-tilt Gb. [2] Therefore, diffusion analysis of polycrystalline grain boundary is performed considering normalized diffusion coefficient as $4.34*10^6$, $2.07*10^6$, and $1.13*10^5$. [16]

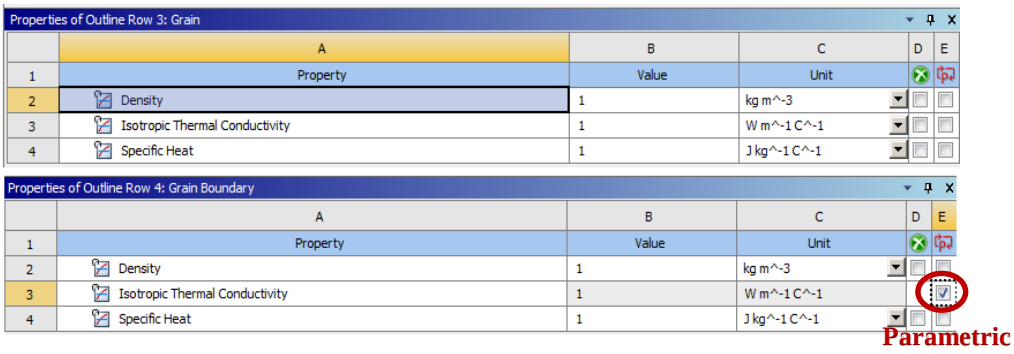

Figure 3.2 Material properties entered in ANSYS workbench.

3.1.3. Modeling

Assigning analysis model, material properties, boundary conditions and defining element type are important in ANSYS. Since the model is 2- dimension axisymmetric, both PLANE55 and PLANE77 can be worked in this case. PLANE77 is 8- Node thermal solid element. The 8-node thermal element is applicable to a two-dimensional, steady-state and transient thermal analysis with temperature as degrees of freedom. In ANSYS Workbench 15.0, PLANE77 element is opted for transient analysis. The modeling and meshing procedure is explained below:

1. List the material properties by defining two material models i.e. grain and grain boundary (GB) in engineering data, as discussed material properties section.
2. Draw 2D polycrystalline grain and GB model in design modular. Even though Grain and GB are considered as separate material, they are part of same system. Hence, one part of two bodies is formed.

3. In modeling part, material properties are assigned to respective geometry. After assigning material fine mapped meshing is applied on both geometries. Since, the geometry is simple mapped meshing is achieved just by refining both geometries up to level 2.
4. It is important to mention that, this mass diffusion problem is initial boundary value problem. Hence, for initial condition temperature is maintained at T=0. This means that, at starting, there is no hydrogen present in the system and it will diffuse along with time.
5. Furthermore, higher concentration (T= 1) is maintained on one side of the system while zero concentration on opposite side of high concentration. For remaining sides, zero heat flux condition is maintained throughout simulations.
6. For transient thermal analysis, it is important to find out diffusion time for given system. It is simple to calculate diffusion time for simple geometry we considered with formula $t = \frac{x^2}{2D}$; where, *x*= diffusion length and *D*= diffusion constant. [18]
7. In order to get fair understanding of diffusion pattern with different diffusion constants, particular time is set for all values of diffusion constants.

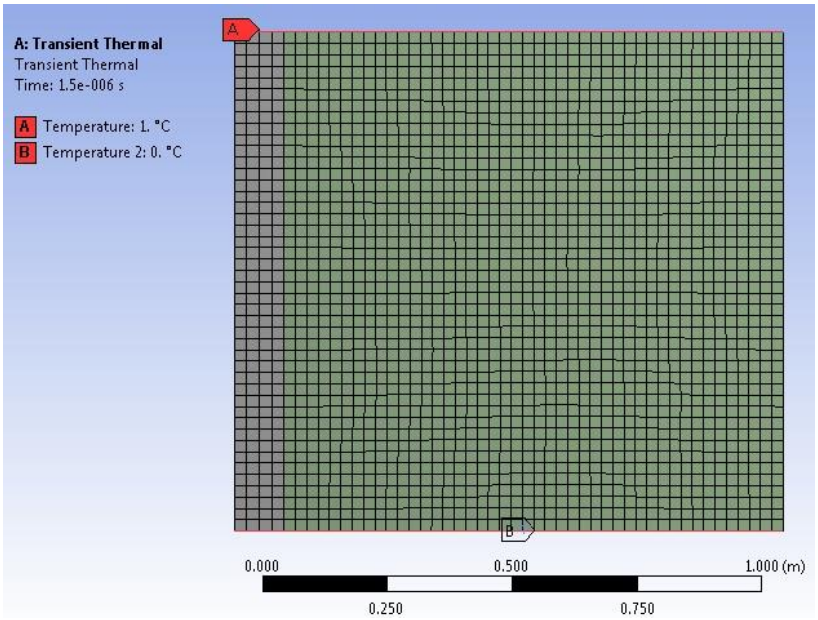

Figure 3.3 Meshing and Boundary condition.

3.1.4. Simulation Results

In this section, several cases of simulation with different diffusion constants and different grain boundary sizes are performed. Figures and plots for each case are discussed accordingly.

Case 1: Polycrystalline grain and Twist GB diffusion constant with different size of Grain boundary.

In this case, normalized diffusivity of grain boundary with respect to magnesium grain is assumed to be $4.34*40^6$. Here, theoretical diffusion time for system is considered as 0.017s. To have clear understanding of concentration pattern, we have taken three simulation patterns at initial time, intermediate time and at final time. Following figures shows how concentration in polycrystalline grain and grain boundary evolve with respect to time. Three different sizes for grain boundaries i.e. 0.1, 0.05, 0.01 are studied.

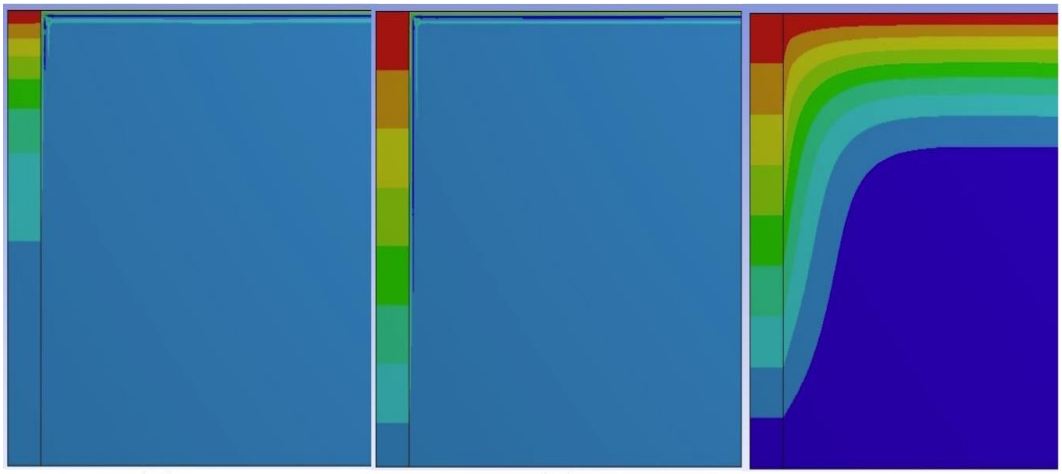

(a)

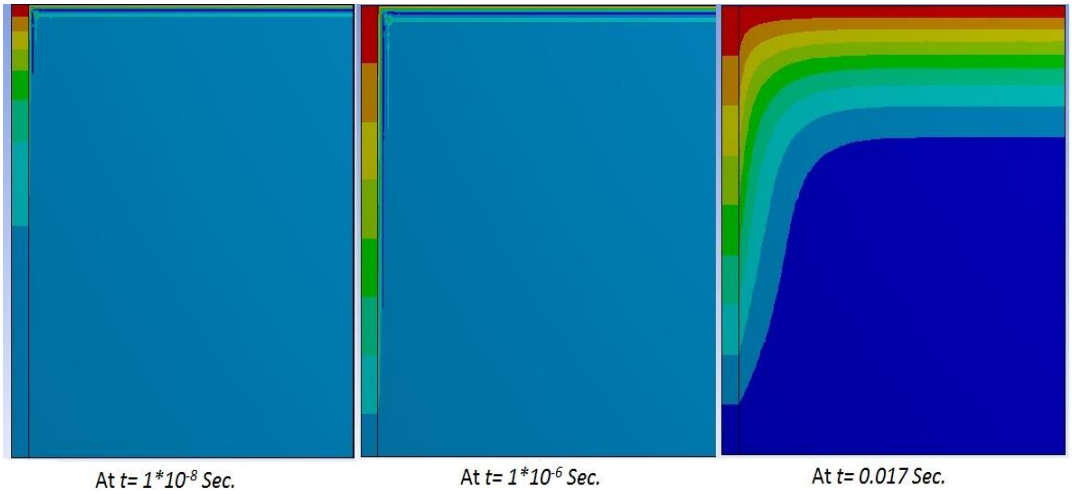

(b)

Figure 3.4 Case 1, (a) Concentration distribution in GB of size 0.1 (b) Concentration distribution in GB of size 0.05.

Case 2: Polycrystalline grain and Tilt GB diffusion constant with different size of Grain boundary.

In this case, normalized diffusivity of grain boundary with respect to magnesium grain is assumed to be $2.073*10^6$. And, theoretical diffusion time for system is considered as 0.017s. Two different sizes for grain boundaries i.e. 0.1, 0.05 are discussed below:

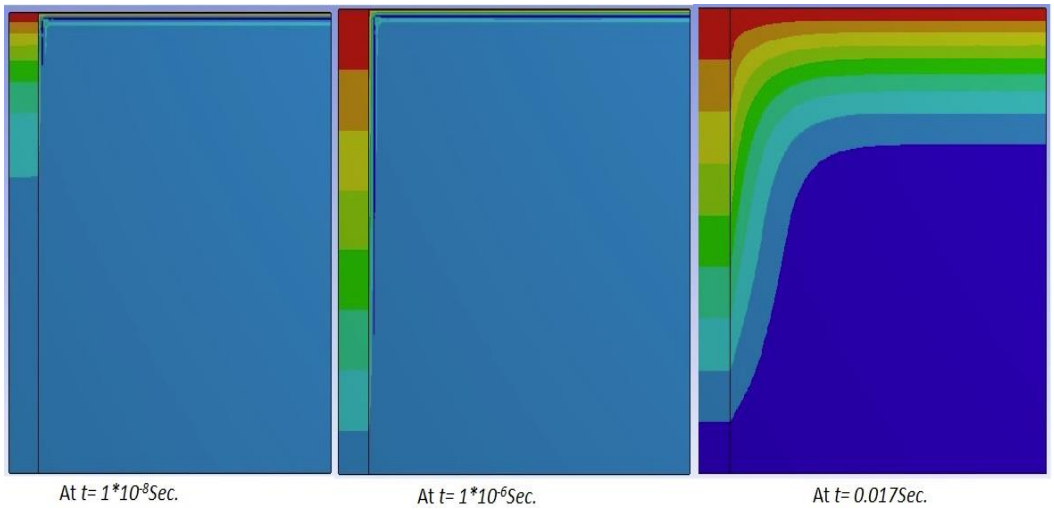

(a)

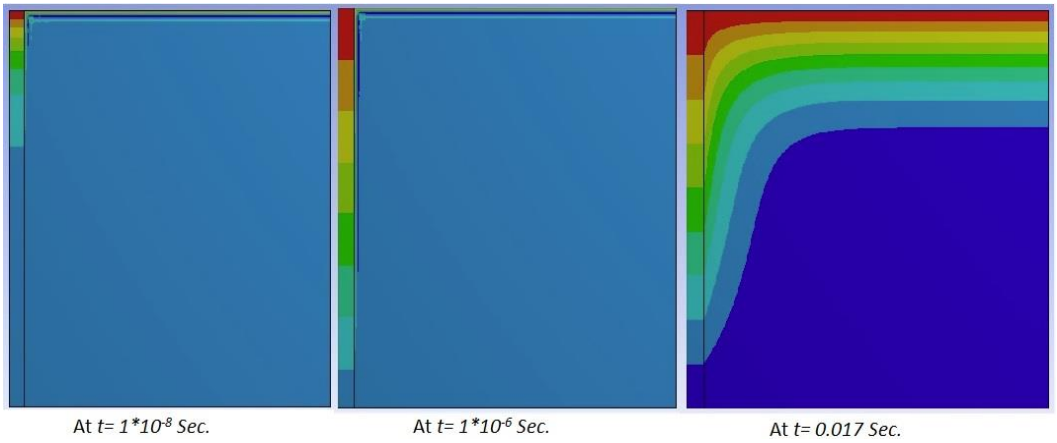

(b)

Figure 3.5 Case 2, (a) Concentration distribution in GB of size 0.1 (b) Concentration distribution in GB of size 0.05.

Case 3: Polycrystalline grain and Twist + Tilt GB diffusion constant with different size of Grain boundary.

In this case, normalized diffusivity of grain boundary with respect to magnesium grain is assumed to $1.13*10^5$. And, theoretical diffusion time for system is considered as 0.017s. Two different sizes for grain boundaries i.e. 0.1, 0.05 are discussed below:

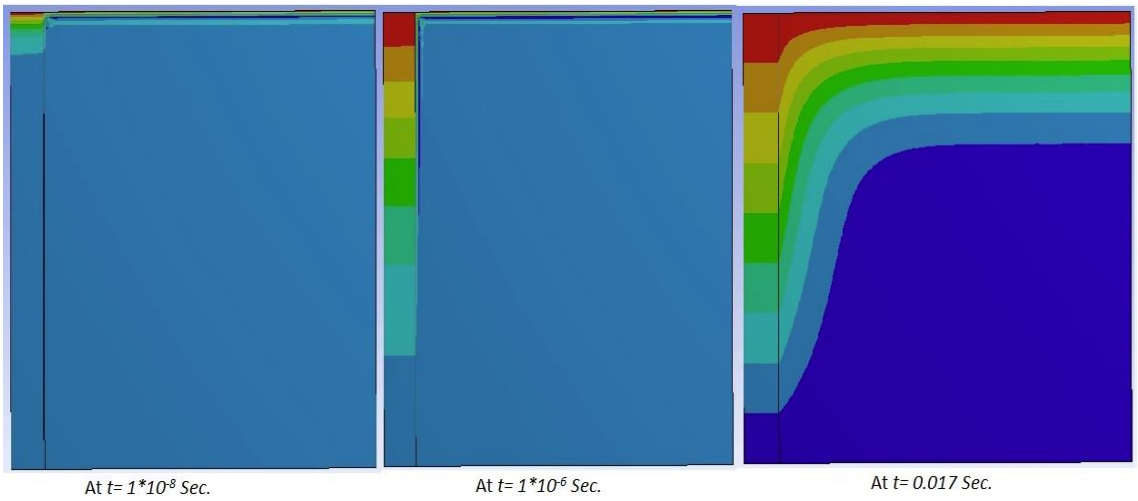

(a)

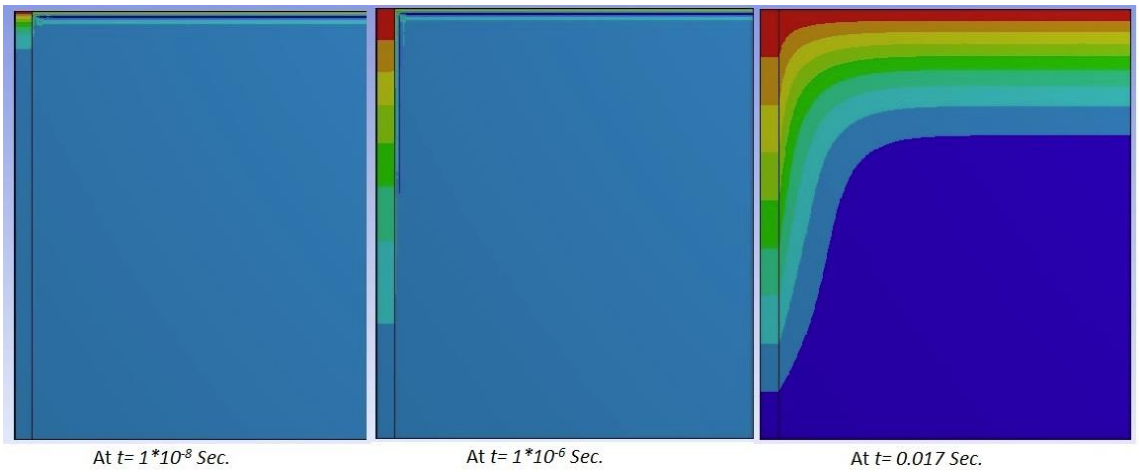

(b)

Figure 3.6 Case 3, (a) Concentration distribution in GB of size 0.1 (b) Concentration distribution in GB of size 0.05.

3.1.5. Discussion

After doing simulations for different cases, it is clear that; greater diffusion coefficient increases the rate of hydrogen to insert in magnesium polycrystalline grain boundary. In this study, diffusion in twist grain boundary type and tilt grain boundary type have almost same diffusion rate at saturation time. While, if we consider initial and intermediate times and see diffusion patterns, there is remarkable difference in both cases. Diffusion in twist GB is definitely more compare to tilt and twist + tilt types of grain boundaries. In real life scenario, there is a combination of all three types of grain boundaries in one multigrain polycrystalline system. Hence, it is important to see how these mismatches affect overall diffusion pattern of multigrain polycrystalline system. Additionally, during the insertion of hydrogen some morphological changes may occur in grain boundary. Further part of this chapter introduces diffusion analysis of multigrain polycrystalline system.

3.2. Multi grain polycrystalline grain and grain boundary composing

In previous part of this chapter, single polycrystalline geometry is considered for diffusion analysis and effective diffusion from grain boundary compares to grain is studied. But, there are many parameters which are responsible for diffusion through grain boundary such as, neighboring grain size, its structure, diffusion constant overall length through which hydrogen is inserted, size and geometry of grain boundary. In order to have strong understanding of hydrogenation and dehydrogenation process, study of single polycrystalline is not well enough. Hence, we have modeled multigrain polycrystalline structure in ANSYS Workbench and simulations are carried out at different time steps.

3.2.1. ANSYS Modeling

For ANSYS modeling, we have taken a reference image of nanocrystalline grain structure of magnesium and modeling is completed with reference to the literature. Step by step description of geometry, modeling and set up is described below:

1. Separate geometry system model is chosen to make geometry in ANSYS Workbench. All the dimensions are normalized with respect to length of first crystal in the geometry and step by step geometry of grain and grain boundary is prepared with reference picture. Reference picture is as shown below. It is difficult to draw with the same dimension as shown in figure 3.2.1.in ANSYS, as the dimensions are in nano and micro level. So, we have assumed normalized dimensions.
2. There are 13 surface areas are created for polycrystalline grain part and total 16 grain boundaries are sketched. For all the polycrystalline grain geometries, one part is made having 13 bodies. Similarly, another part is formed which has 16 bodies represents grain boundaries.

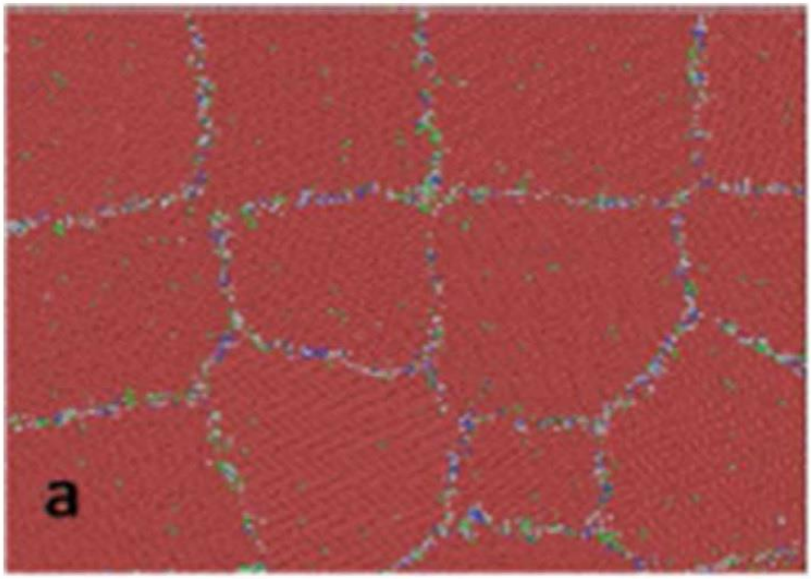

Figure 3.7 Reference for polycrystalline magnesium grain structure. [15]

3. After completion of geometry, new analysis model is used to do transient diffusion analysis. Material properties are considered same as that of single crystal geometry.
4. In multigrain geometry, there are different types of grain boundaries present with different diffusion constants as discussed individually in previous part. Different material properties assigned to different grain boundaries.
5. After assigning material fine mapped meshing is applied on both part of geometries. Since, the geometry is not symmetrical, plain stress condition is maintained. And fine meshing is applied to both parts. To get accurate results in grain boundaries, element size of 0.08 is maintained on grain boundary face.
6. Continuity is maintained between grain and grain boundary by executing suitable contact meshing at the grain and grain boundary.
7. Boundary conditions are maintained same as that of single polycrystalline model. And initial concentration is maintained zero.
8. Simulations results for different cases are discussed in following part.

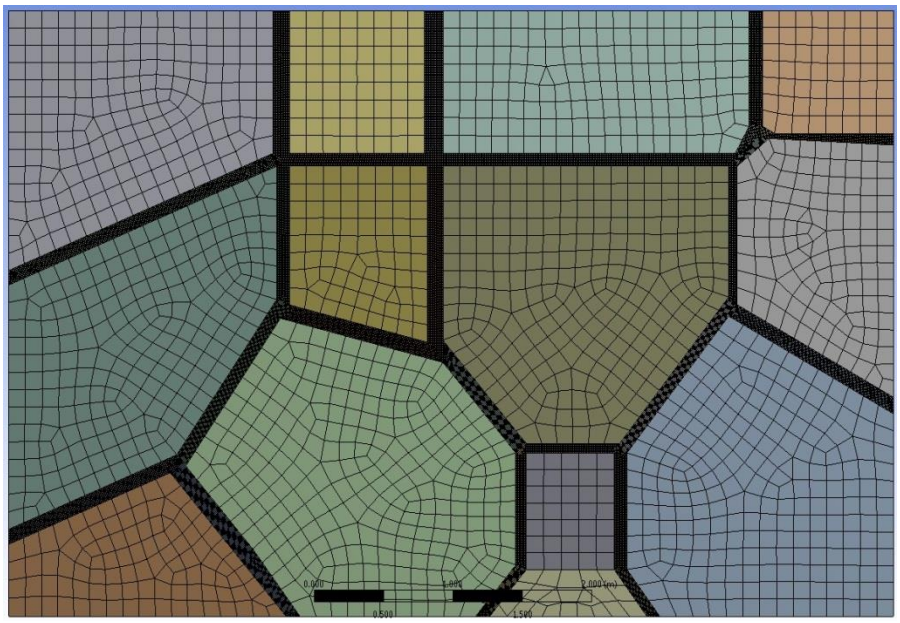

Figure 3.8 Actual geometry created in ANSYS Workbench.

3.2.2. Simulation Results

When hydrogen is inserted at initial time, concentration distribution is as shown in below.

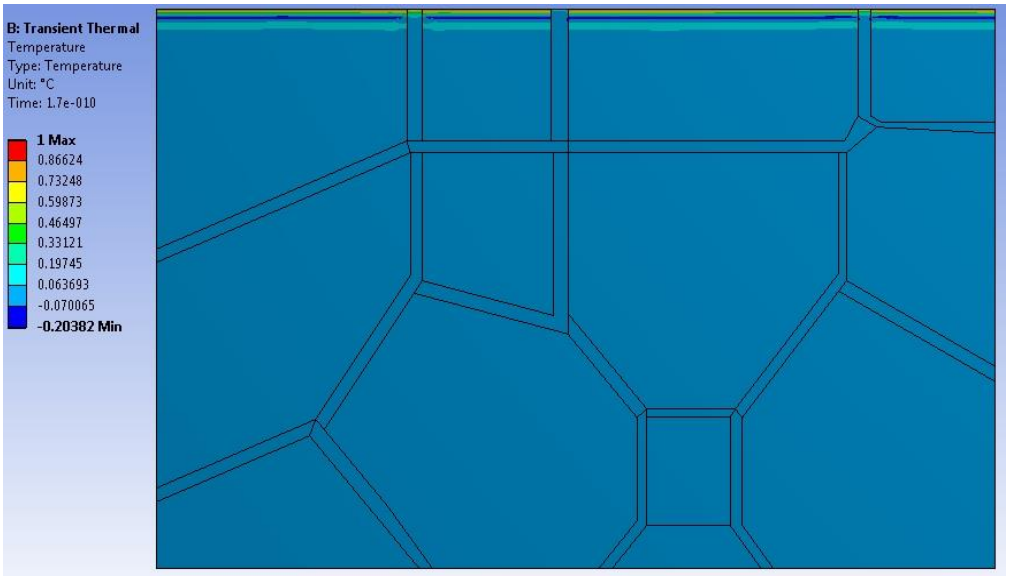

Figure 3.9 Concentration distribution at initial time, t= 1.7*10-10sec.

At this time, overall concentration of hydrogen is negligible in both grain and grain boundary. As soon as the time increases, hydrogen starts inserting through grain boundary first and then eventually through the grains. This is illustrates in following figure.

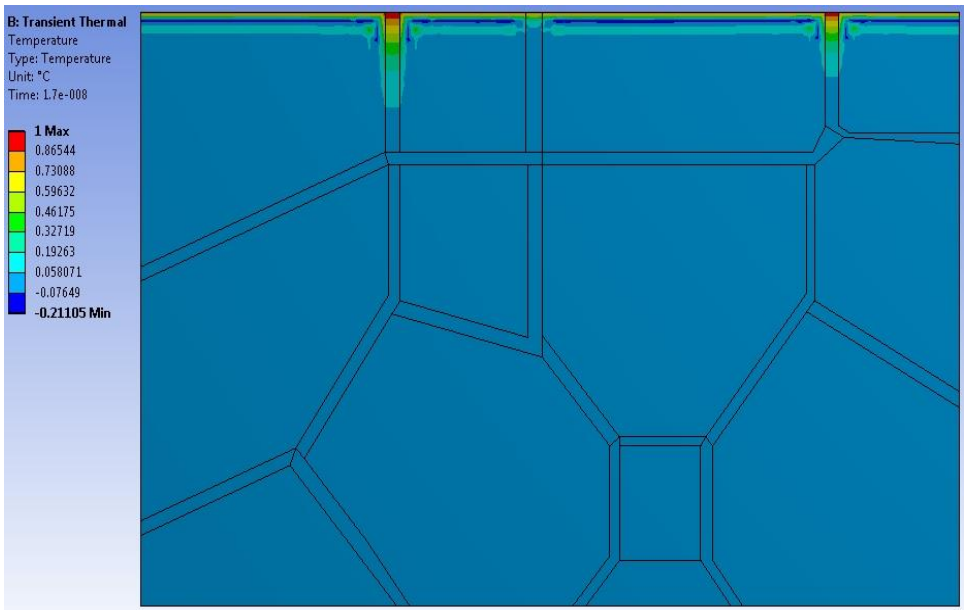

Figure 3.10 Concentration distribution at time, t = 1.7*10-8 sec.

In above snap shot, we can clearly see that the hydrogen through grain boundaries having twist and tilt grain boundary diffusion coefficient passes more as compare to grain boundary having diffusion coefficient of mixed type. But this pattern will not be continues throughout the geometry as, there might be grain boundaries having low diffusion coefficient linked to the grain boundary having higher diffusion coefficient. We have carried out the simulation process for same time as that of single crystal geometry so that comparative study of diffusion process could be possible.

Finally, at time, t= $1.7*10^{-3}$sec, concentration of hydrogen through grain and grain boundary is shown in figure 3.2.2.3. Although at starting diffusion through grain boundary attached to right most grain was low compare to grain boundary attached to left one, eventually due to dissimilar distribution of diffusion coefficient throughout the system, at

final time step, hydrogen passing through the left side grain boundaries of overall structure become more than other side.

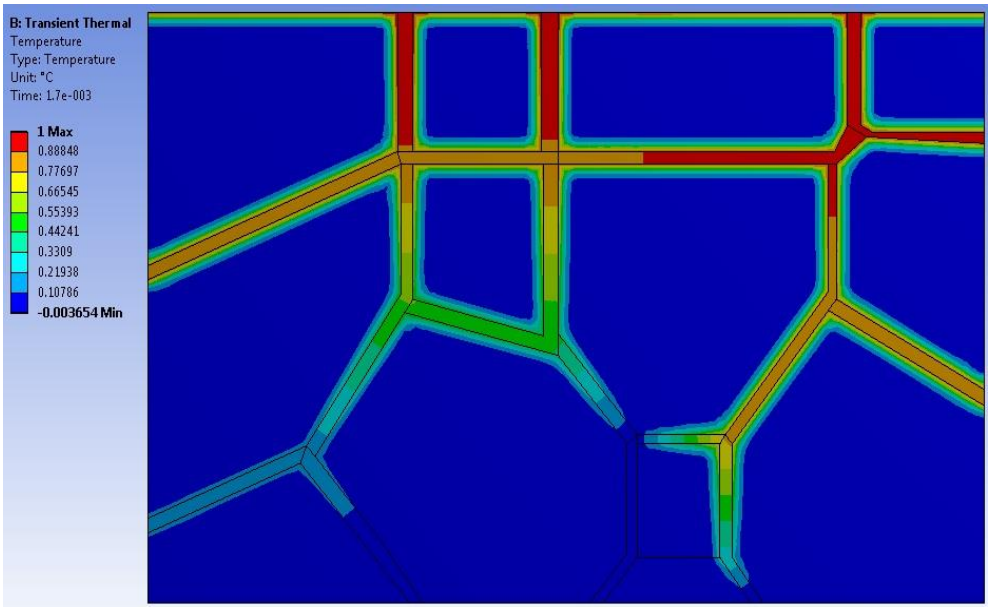

Figure 3.11 Hydrogen distribution at time, t= 1.7*10-3sec.

3.2.3. Discussion

It becomes clear that, diffusion coefficient and type of grain boundary plays significant role in accelerating diffusion process within magnesium bed structure. Moreover, higher the coefficient of diffusion more will be the rate of diffusion. Therefore, it is necessary to have grain boundary in magnesium nano crystalline structure. It is also important to mention that, size of grain boundary does not affect rate of diffusion. In addition to this, size of grain boundary affect its strength of holding hydrogen into it. Hence, it is necessary to have structural analysis of polycrystalline grain – grain boundary system during charging – discharging process. In following chapter, elasto plastic analysis of single grain and multi grain polycrystalline system due to chemical expansion is performed. In this way, we can get clear picture of effective diffusion of hydrogen through grain boundaries.

Chapter 4

CHEMOELESTOPLASTIC ANALYSIS OF POLYCRYSTALLINE MAGNESIUM NANOSTRUCTURE.

Structural analysis of polycrystalline grain and grain boundary can be solved numerically by applying finite element method. The commercial finite element software ANSYS Workbench 15.0 is used to develop the required model. In this chapter, structural aspect of grain boundary is discussed. Chapter gives idea about element selected and meshing considerations, material properties for chemo stress analysis. After that simple model is developed to understand the effect of concentration on GB and how plasticity induced in grain boundary region. Furthermore, multigrain polycrystalline model from Chapter 3 is considered for chemo stress phenomenon.

According to literature study, when hydrogen is inserted in to magnesium grain during hydrogenation, there is chances of high stress induced during this process. This can cause deformations in grain boundaries. There may be the chance of crack incudes in vicinity of grain and grain boundary area. This may cause damage to overall system and can reduce capacity to accommodate hydrogen in nanocrystalline magnesium. Hence, it is important to have insight about morphological changes during charging and discharging process.

4.1. Chemoelestoplastic analysis of single polycrystalline structure

In this part, we will discuss about ANSYS Model, its linking with the transient diffusion analysis performed in previous chapter, material properties considered, meshing parameter for simple geometry. After that, parametric results for elastoplastic analysis are discussed considering yield strength as an input parameter.

4.1.1. ANSYS Model for Structural Analysis

It needs to clarify that this chemical stress problem is mathematically identical to a thermal stress problem. So the hydrogenation process is treated as thermal process in ANSYS simulation. Geometry is considered same as that of transient diffusion analysis model. Nodal results for concentration distribution at particular time step are taken as an input as a thermal condition. In simple case, if we consider a real life situation, polycrystalline magnesium is attached to other magnesium grain, grain boundary or dislocations. We have considered free body motion to achieve most realistic results. ANSYS Workbench 15.0 allows simulating model in free condition. ANSYS adds weak spring forces to unconstrained body to attained solution.

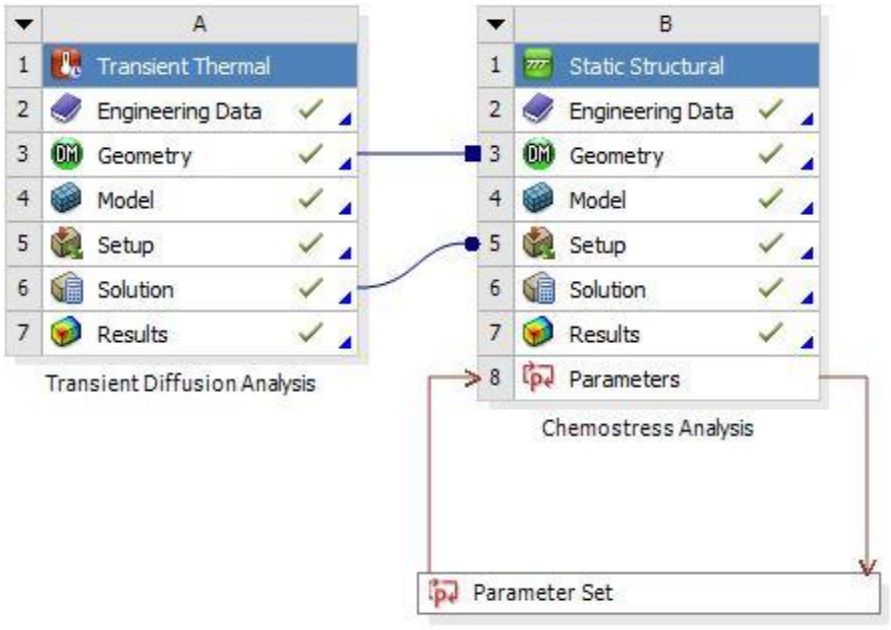

Figure 4.1 ANSYS Model Selection

4.1.2. Material Properties

In this project, material properties are all defined as a bilinear isotropic. To avoid computational errors at Nano to micro scales, all the stresses and material properties are normalized by young's modulus of Magnesium polycrystalline grain. Yield strength of grain boundary is interesting factor to see stresses are varied with respect to change in yield strength. Hence, normalized yield strength of grain boundary is set as an input parameter for parametric study. [16] [20]

$$E_G = 1 \qquad E_{GB} = 0.33$$

$$\nu_G = 0.29 \qquad \nu_{GB} = 0.29$$

$$\sigma'_G = 0.048 \qquad \sigma'_{GB} = 0.024$$

$$\alpha_G = 0.40456 \qquad \alpha_{GB} = 1*10^{-11}$$

$$H_G = 0.1 \qquad H_{GB} = 0.1$$

Where, suffix notation 'G' represents grain and 'GB' represents grain boundary. E is young's modulus, ν denotes Poisson's ratio, σ' denotes yield strength, α is chemical expansion coefficient and H is strain hardening ratio.

4.1.3. Modeling

Simple geometry from diffusion analysis is considered with grain boundary of normalized size of 0.05L. For thermal stress problem, element type selected is PLANE 183 axisymmetric. Thickness for both geometries is given as 1unit.

It is important to have fine mesh near grain and grain boundary contact area. Mapped Face meshing is applied with quadrilateral method. Length of Grain boundary is divided in to 20 numbers of divisions and height is divided in to 100 parts. This meshing yields relatively accurate results. For polycrystalline grain, we can predict from chemical diffusion results that, there will not be significant impact on structure due to hydrogen

insertion. Because, hydrogen will first diffuses completely through the grain boundary. Figure 4.1.3 shows meshing and imported loads in model.

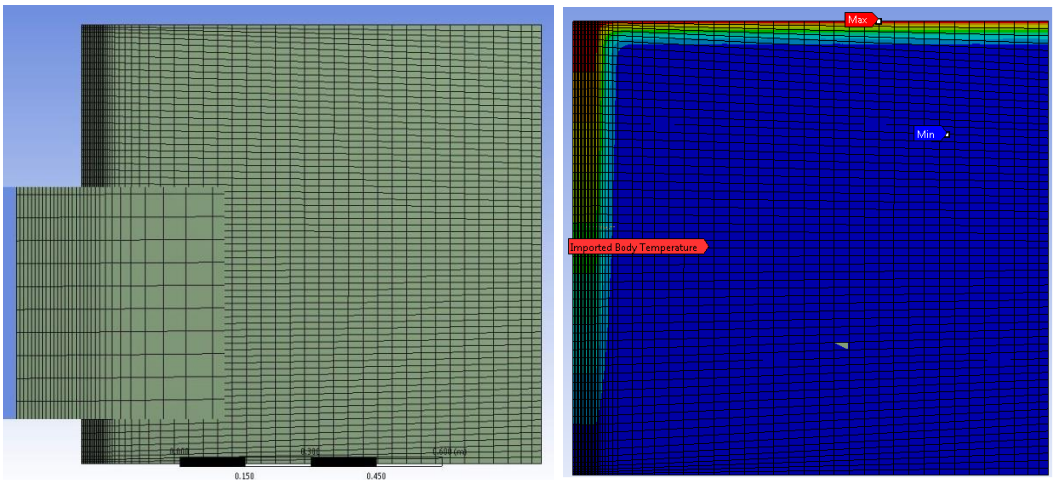

(a) (b)

Figure 4.2 (a) Model Entity and (b) Temperature loads imported on model.

4.1.4. Results and discussion for Single polycrystalline model

In this section, several trials of simulations with different time steps in diffusion process are performed. The results at our area of interest are discussed and compared with each other. Figures and plots give fair idea of how elasto-plasticity induced during hydrogenation process.

4.1.4.1. Equivalent Stress and Deformation

Step by step analysis of grain- grain boundary contact is shown below. Initially, there is no significance of deformation or stresses induced in the Grain- Grain boundary region. As soon as hydrogen inserted in to the polycrystalline grain, there is an evidence of highest stress on the contact of grain and grain boundary. As hydrogen diffuse through grain boundary, the stress on the contact region increases significantly. Following figure shows how stress induced as the diffusion process walk in time. After certain time stresses induced in contact stops increasing

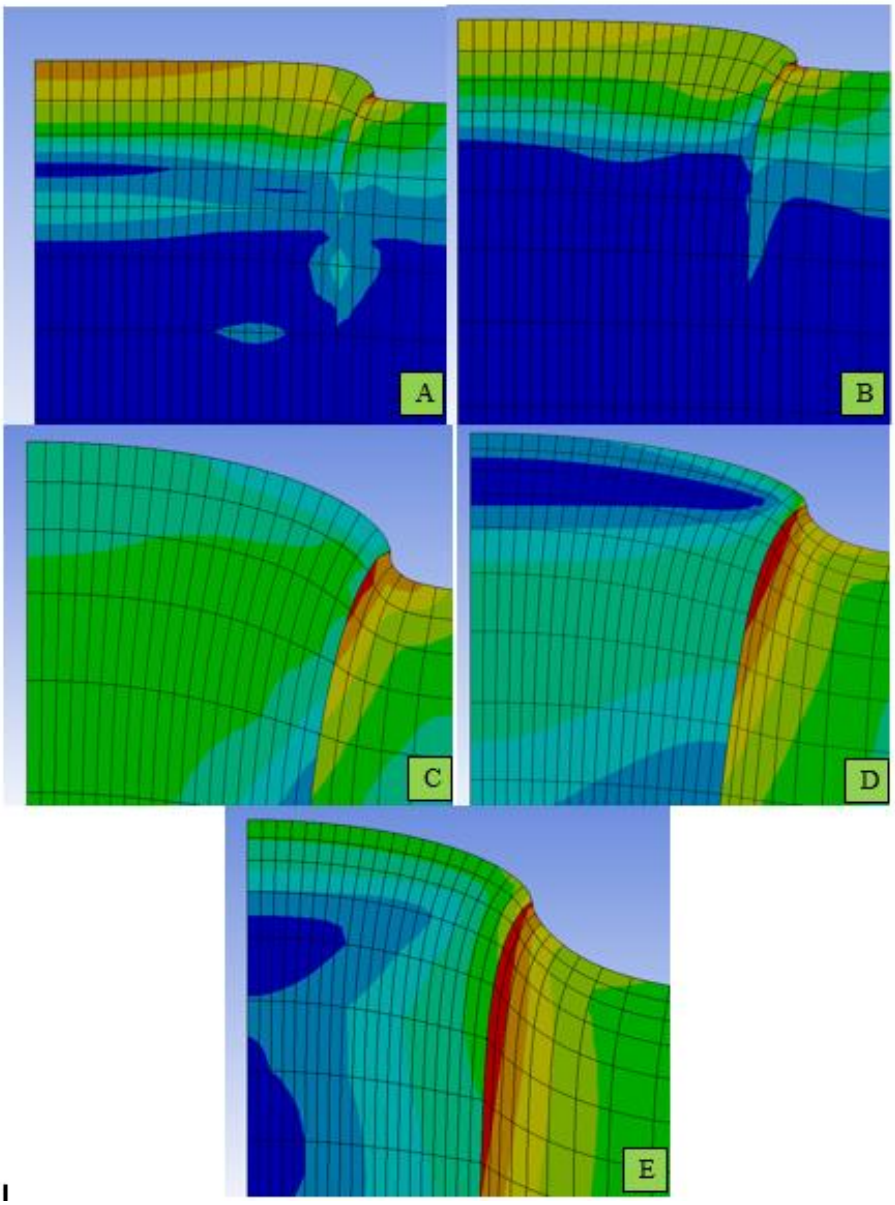

Figure 4.3 Isotropic contour plots of von misses stresses at (A) t= 1.7e-10sec. (B) t= 1.7e-9sec. (C) t= 1.7e-8sec. (D) t= 1.7e-7sec. (E) t= 1.7e6sec.

The snapshot showed below is result of equivalent (Von-Mises) stresses induced after the grain boundary is fully hydrogenated with hydrogen.

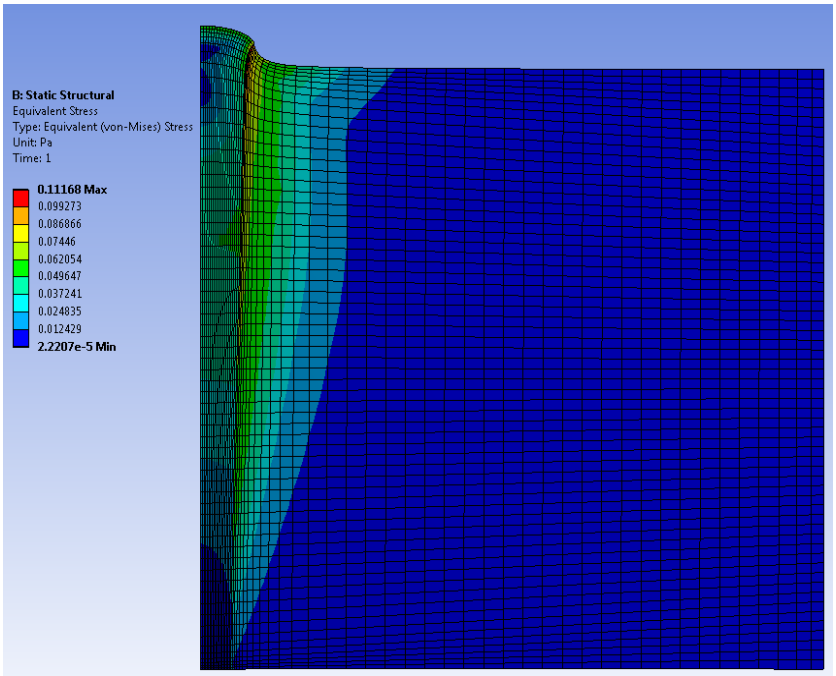

Figure 4.4 Isotropic contour plot of equivalent stresses in overall system after fully charged condition on True Scale (1.0).

It is interesting to study that, after time 1.710^{-5} sec. there is no change in stresses throughout the system as shown in figure 4.1.4.4. Moreover, maximum stress values are above yield strength of polycrystalline grain and grain boundary. Maximum stresses are induced at the initial contact between grain and grain boundary. It seems to be clear explanation that, when hydrogen continuously inserted from the same region, it is obvious to have large amount of stresses should be induced in that region. Moreover, the contact between grain and grain boundary goes in to plastic region and permanent deformation takes place during insertion of hydrogen. This can increase the overall size of grain boundary and allows having more hydrogen diffusion through the grain boundary. This can results in better charging and discharging rate. Although, there is increase in size of grain boundary, it is important that the grain boundary should not generate the crack.

Formation of cracks may damage to the system and it will significantly reduce charging and discharging rate.

Following graph shows the variation of maximum stress induced in the overall system as diffusion process march in time.

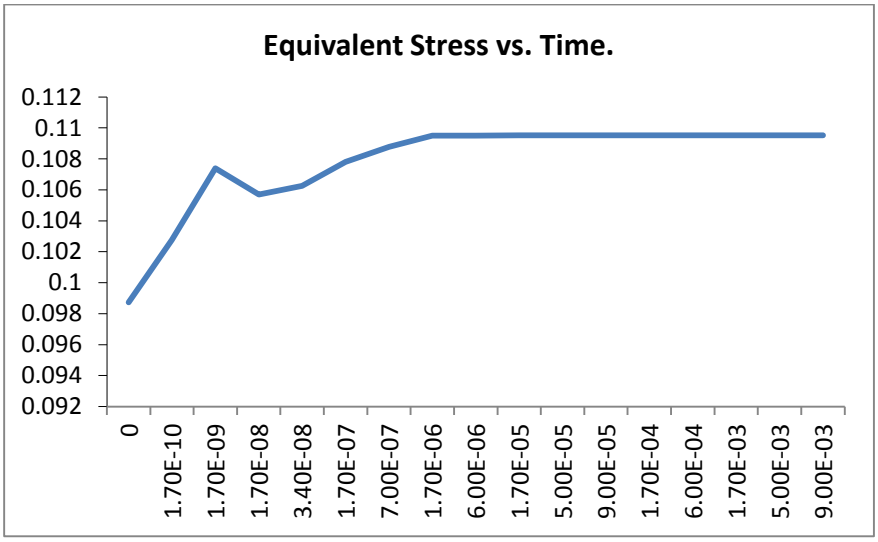

Figure 4.5 Maximum equivalent stress at different time steps during diffusion.

During hydrogenation process, if we observed total deformation (Maximum total deformation) in the system, it is basically in the region of contact between grain and grain boundary. From following graph we can see that, after first time elapsed, maximum total deformation increases for next times gradually up to $6*10^{-6}$ sec. and after that same deformation occurs at every time.

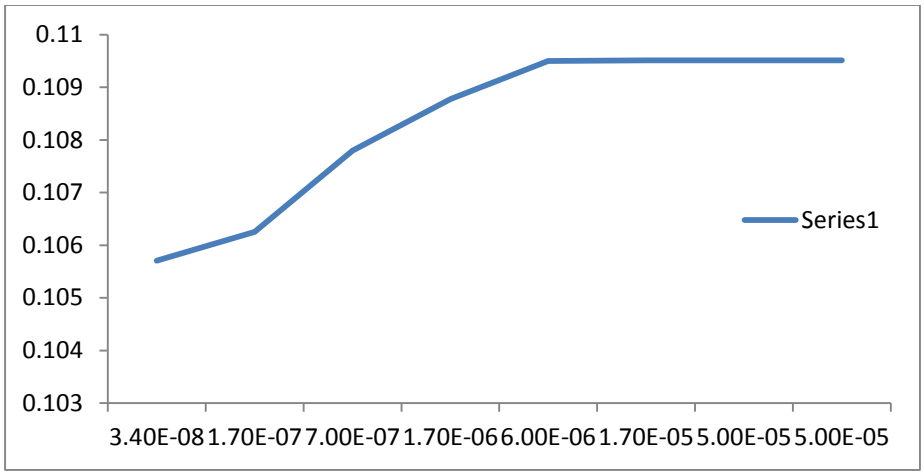

Figure 4.6 Maximum total deformation at different time steps during diffusion.

Following two snapshots show the total deformation and directional deformation in y- direction after fully charged condition respectively.

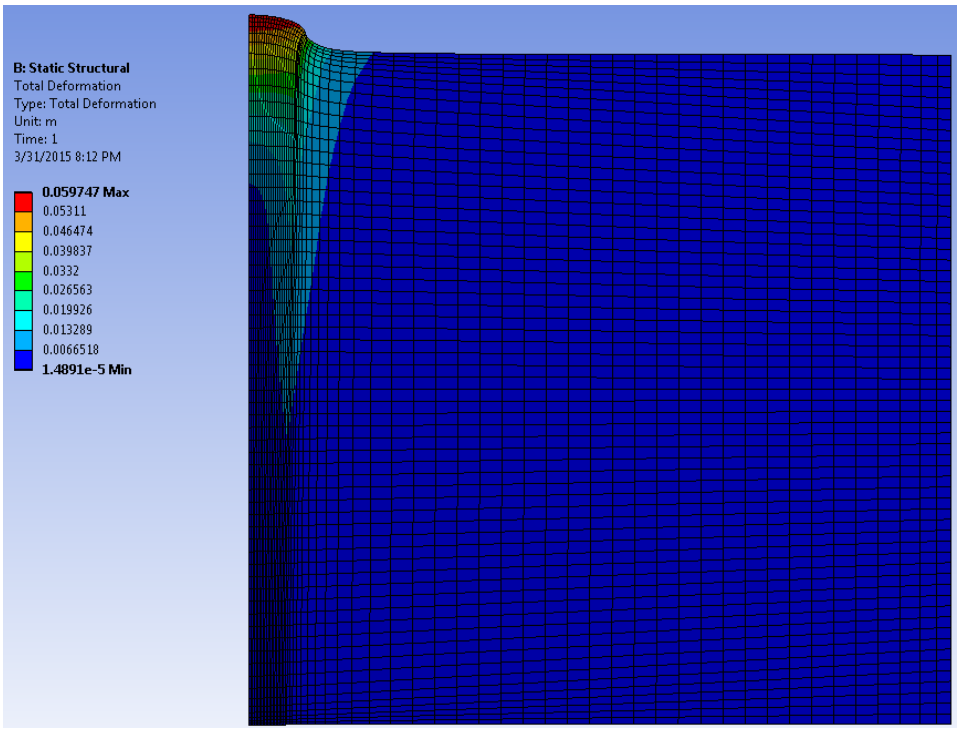

Figure 4.7 Total deformation after fully charged condition.

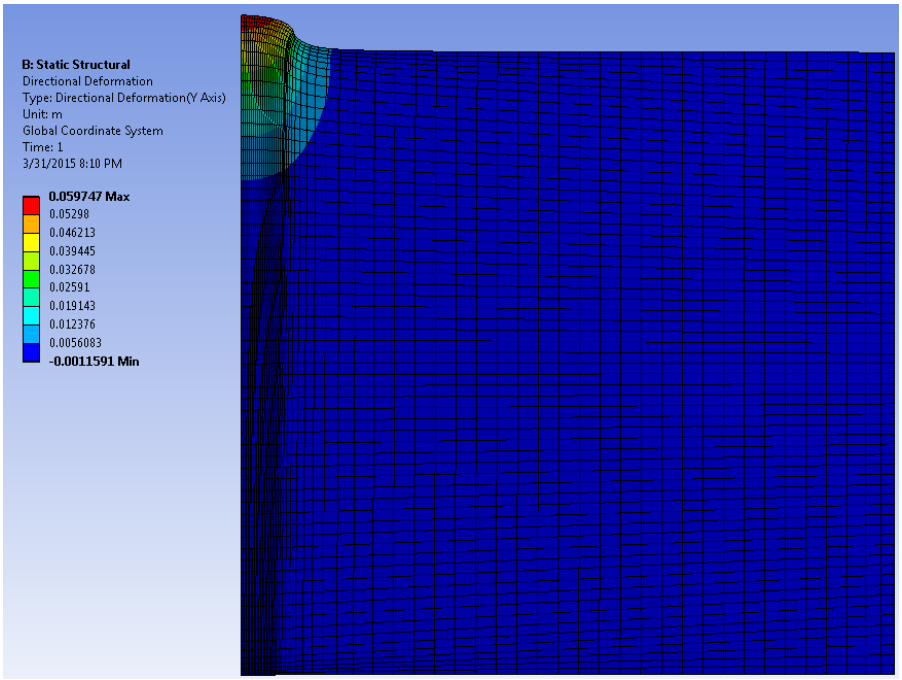

Figure 4.8 Directional Deformation (Y- axis) after fully charged condition.

4.1.4.2. Equivalent Plastic Strain

Plastic deformation results from slip between planes of atoms due to shear stresses. This dislocation motion in polycrystalline grains/GBs is essentially due to atoms in the crystal structure rearranging themselves to have new neighbors. This results in unrecoverable strains (Plastic strain) or permanent deformation in grain boundaries after hydrogen atom passed through certain location. It is always important have this type of swelling in grain boundaries. This could help in fast moving of hydrogen during charging/ discharging process and increase overall efficiency of hydrogen storage. Following figure shows overall plastic strain induced in single crystal geometry when magnesium nanocrystal is in fully charged condition.

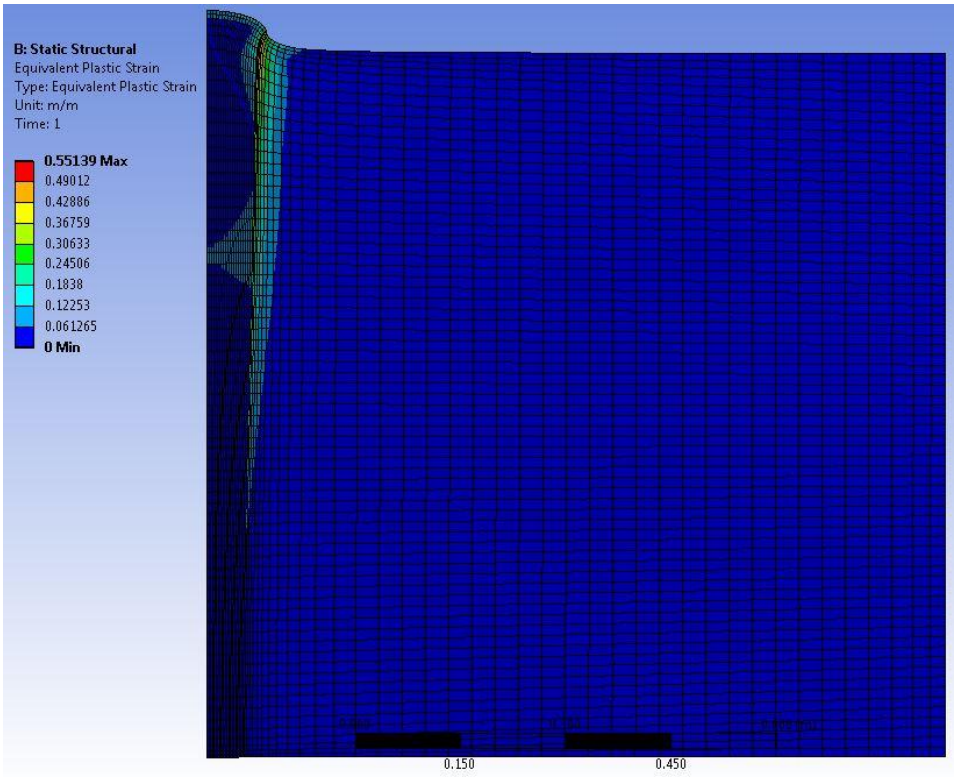

Figure 4.9 Equivalent plastic strain at fully charged condition True Scale (1.0).

4.1.5. Discussion for different yield strength of Grain Boundary

To further study the plastic strain in a grain boundary having different yield strength, four set of simulations with different yield strength of grain boundary are performed. The yield strength σ'_{GB} equals to 0.75 σ', 0.25 σ'_G, 0.05 σ'_G, 0.025 σ'_G. Parametric analysis is performed in ANSYS Workbench. The nodal solution which have maximum plastic strain values at each time are set to compare. Also, elements near contact of grain and grain boundary are examined.

4.1.5.1. The yield strength $\sigma'_{GB} = 0.75\ \sigma'_G$

When yield strength of grain boundary is set to 0.75 that of polycrystalline grain, plastic stain during the initial steps increases in polycrystalline grain. It is interesting to note that, only polycrystalline grain undergoes plastic strain and overall structure of grain

boundary does not affect much. Following figures shows time to time increase in plastic strain on overall geometry.

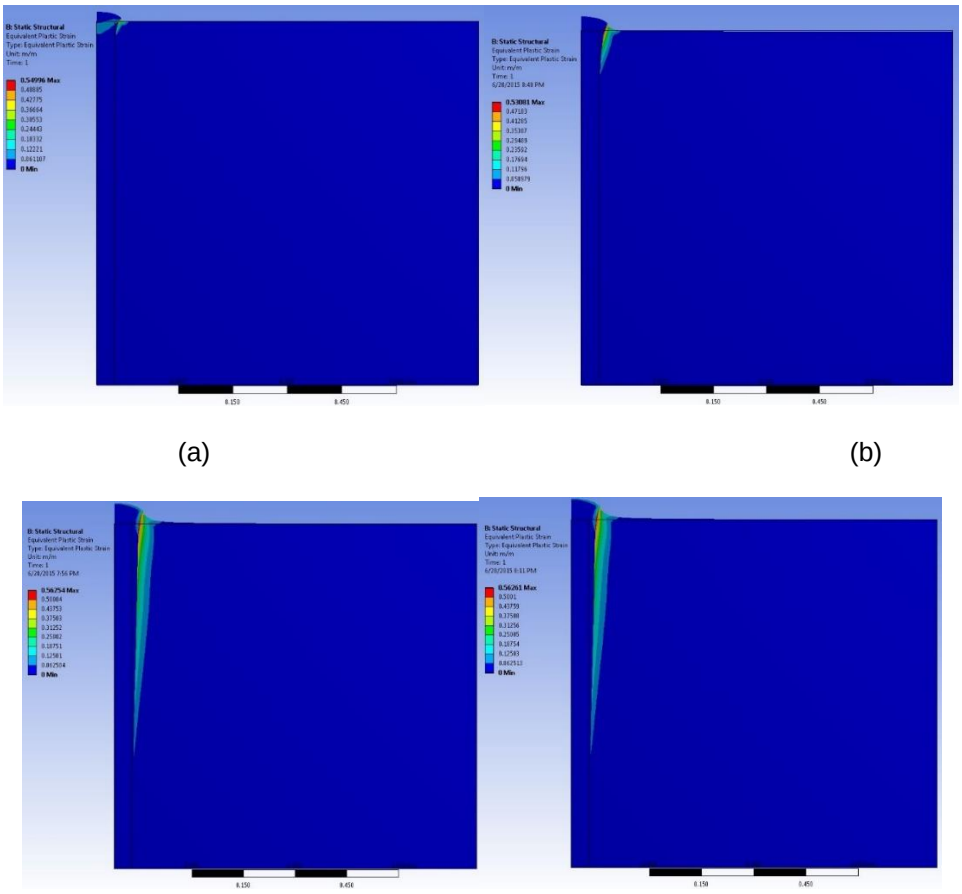

(a) (b)

(c) (d)

Figure 4.10 Equivalent plastic strain (σ'GB = 0.75 σ'G) when, (a) t= 1.7e-10sec. (b) t= 1.7e-8sec. (c) t= 1.7e-7sec. (d) t= 1.7e-2sec

4.1.5.2. The yield strength $\sigma'_{GB} = 0.25\ \sigma'_{G}$

When yield strength of grain boundary is set to 0.25 than that of polycrystalline grain, plastic strain during the initial steps increases in polycrystalline grain. Here, plastic strain induced in both grain and grain boundary. Significant increase in plastic strain can be seen in starting steps. This leads in swelling of grain boundary during charging-

discharging process. Following figures shows time to time increase in plastic strain on overall geometry.

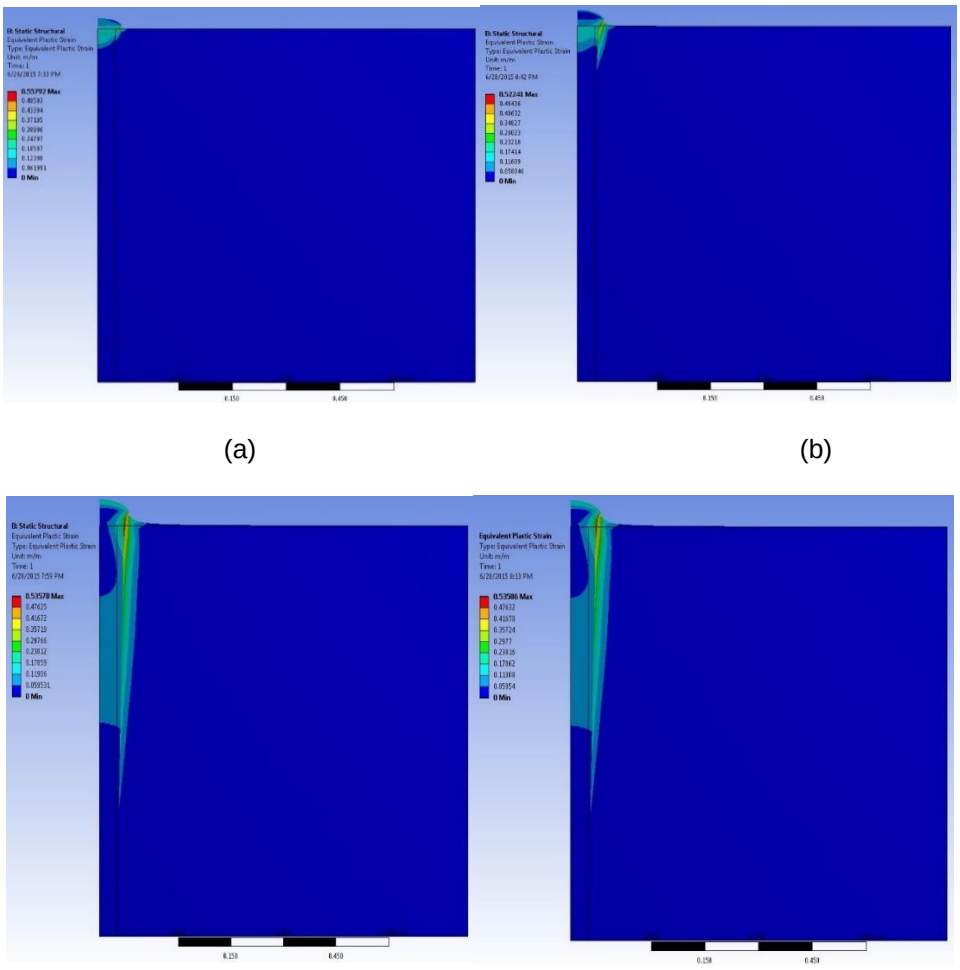

(a) (b)

(c) (d)

Figure 4.11 Equivalent plastic strain (σ'GB = 0.25 σ'G) when, (a) t= 1.7e-10sec. (b) t= 1.7e-8sec. (c) t= 1.7e-7sec. (d) t= 1.7e-2sec

4.1.5.3. The yield strength $\sigma'_{GB} = 0.05\sigma'_{G}$

When yield strength of grain boundary is set to 0.05 than that of polycrystalline grain, plastic strain during the initial steps increases in polycrystalline grain. It is important to mention that, change in yield strength of grain boundary from 0.25 to 0.05 not affect

significantly on overall structure. Step by step increase in plastic strain is shown in following images.

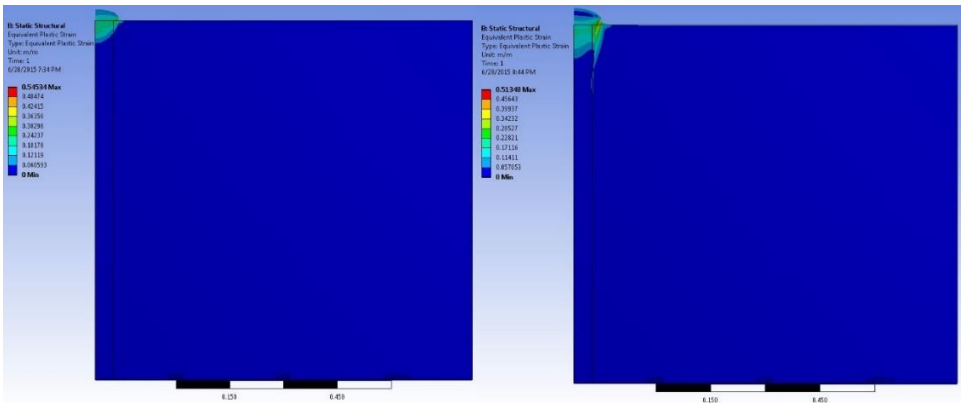

(a) (b)

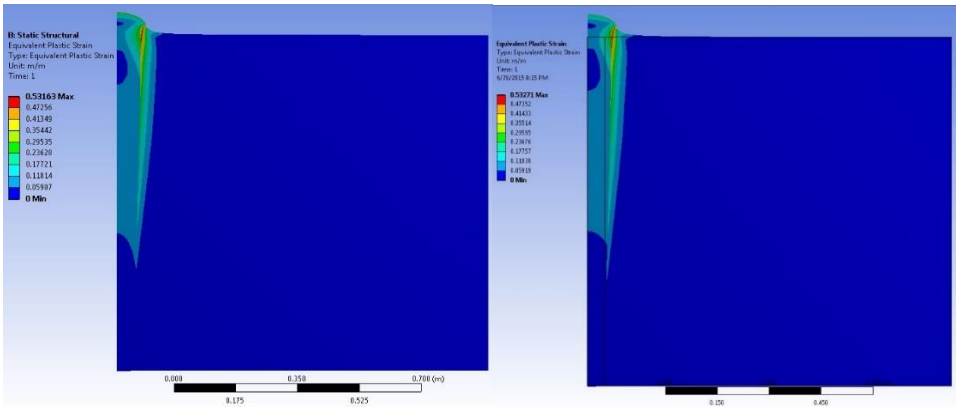

(c) (d)

Figure 4.12 Equivalent plastic strain (σ'GB = 0.05 σ'G) when, (a) t= 1.7e-10sec. (b) t= 1.7e-8sec. (c) t= 1.7e-7sec. (d) t= 1.7e-2sec

4.1.5.4. The yield strength $\sigma'_{GB} = 0.025\sigma'_{G}$

When yield strength of grain boundary is set to 0.025 than that of polycrystalline grain, following results are captured during simulation. In this case, plastic strain at time step 1.7e-8 is more compared to all other parameters. Final structure of grain boundary

remains same as that of other parameters. Step by step increase in plastic strain is shown in following images.

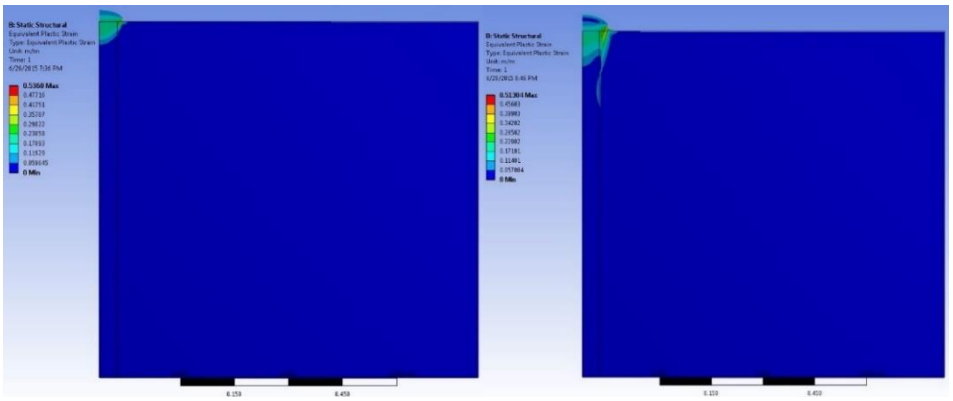

(a) (b)

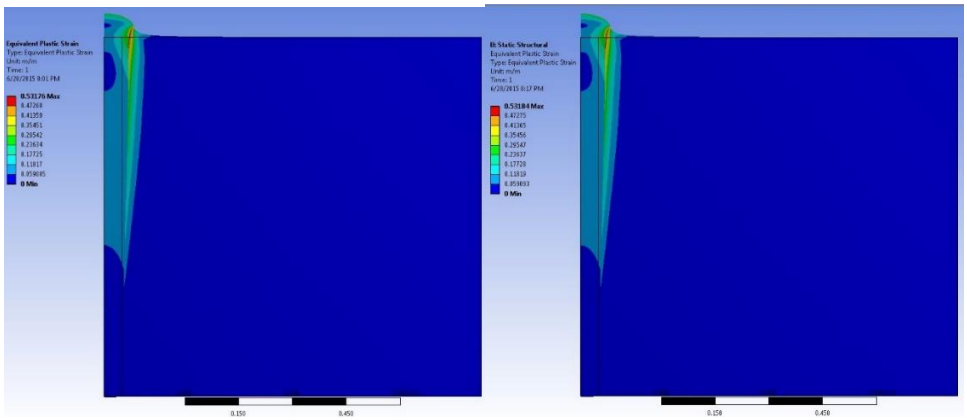

(c) (d)

Figure 4.13 Equivalent plastic strain (***σ***'GB = 0.025 ***σ***'G) when, (a) t= 1.7e-10sec. (b) t= 1.7e-8sec. (c) t= 1.7e-7sec. (d) t= 1.7e-2sec

This parametric study on single polycrystalline grain – grain boundary structure gives idea about exact yield strength of grain boundary to be achieve in order to have better hydrogenation/dehydrogenation process. It is always important to have better strength of grain boundaries during hydrogenation process. As, more grain boundaries can expand more will be the chances of flowing hydrogen through it. We can see from graph below that

highest equivalent plastic strain induced in grain boundary which has yield strength of 0.75 of grain. This expansion is mainly in polycrystalline grain. However, if yield strength of grain boundary is 0.025 of polycrystalline grain, it gives more expansion in GB as well as polycrystalline grain, which is important for fast charging process. In addition to this, overall strength of grain boundary is maintained having strength of 0.025 yield strength. Experimental data needs to support this study. Other parameters such as directional deformation, von – Mises stress and von – Mises strain does not have significant changes with change in yield strength of grain boundary.

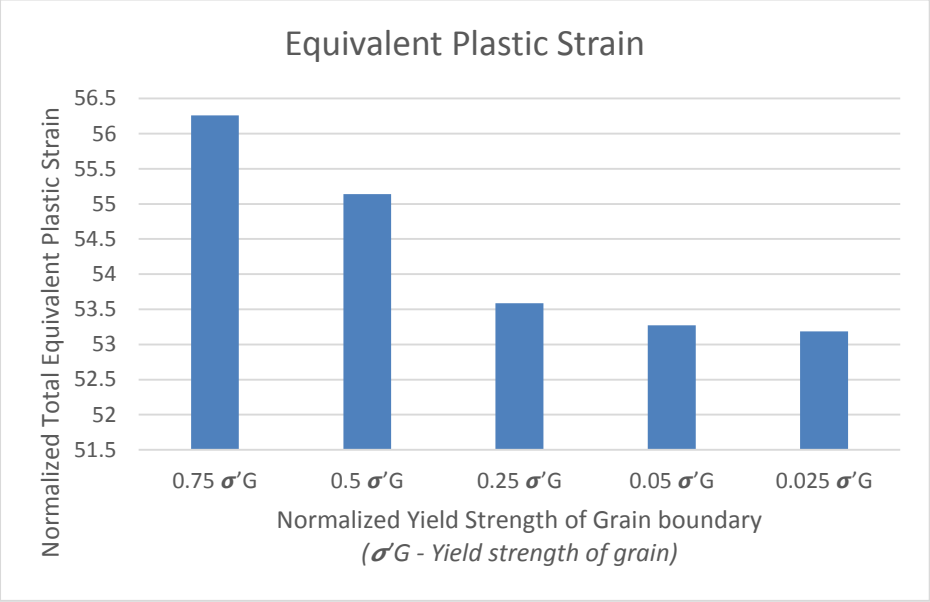

Figure 4.14 Parametric analysis result for different types of grain boundaries.

Analysis of single polycrystalline grain gives central idea about chemical stresses induced during hydrogenation. However, it is essential to have comprehensive idea in real life situation which have multigrain polycrystalline structure. Complex magnesium nanostructure have combination of grains having different diffusion coefficients, types and sizes. In following section, chemical stresses induced in multigrain polycrystalline structure is discussed.

4.2. Chemoelestoplastic analysis of multigrain polycrystalline structure.

As we have seen in previous chapter that complex geometry gives completely different picture of hydrogen diffusion through multigrain polycrystalline Mg nanostructure. In this part, we will take a look at chemical stresses induced during charging process and how it affects overall structure.

4.2.1. ANSYS Model for Structural Analysis

For chemo – stress analysis, geometry is imported from multigrain diffusion analysis. As ANSYS has different model for chemo stress analysis (thermal stress analysis in ANSYS) meshing steps are different than diffusion model. Step by step description of geometry, modeling and set up is described below:

9. In multigrain geometry, there are different types of grain boundaries present with different diffusion constants as discussed in previous chapter. Different diffusion properties assigned to different grain boundaries.
10. Structural material properties and element type are considered same as that of single crystal geometry.
11. After assigning material face sizing meshing is applied on both grain and grain boundary. On grain boundaries, face sizing is maintained at $2e^{-2}$ m element size while on grain structure, it is 5e-2 m. additionally, element behavior is soft. The reason behind fine meshing of grain boundary is to have precise result at grain boundary. Continuity is maintained between grain and grain boundary by executing suitable contact meshing at the grain and grain boundary.

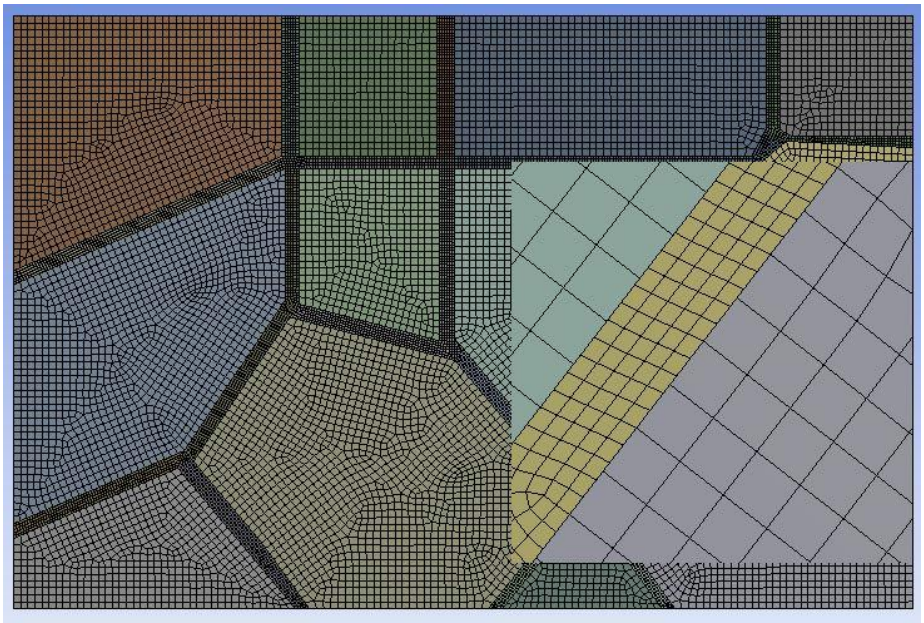

Figure 4.15 Meshing Pattern for Structural analysis of Multigrain structure.

12. Boundary conditions are maintained same as that of single polycrystalline model. Simulations results for different cases are discussed in following part.

4.2.2. Results and discussion for Multigrain polycrystalline model

In this section, structural effect of hydrogen insertion at different time steps in multigrain magnesium nanostructure are discussed. This problem is theoretically similar to thermal stress problem

4.2.2.1. Total Von-Mises Stresses

The step by step analysis of total von mises stresses induced in system is discussed with reference to ANSYS Simulation. Stresses are gradually increase in overall system as hydrogen inserted in Magnesium nanostructure. The crucial area where stresses are induced is near grain boundaries. Total diffusion time for hydrogen is considered as 1.7 e^{-2}sec. During this period, significant increase in stress is up to 1.7e^{-}

^{5}sec. After this step, overall system tend towards saturation phase and system does not show significant increase in equivalent stress. Following images shows stress pattern with respect to time. In ANSYS, all results are analyzed on 1.0 true scale.

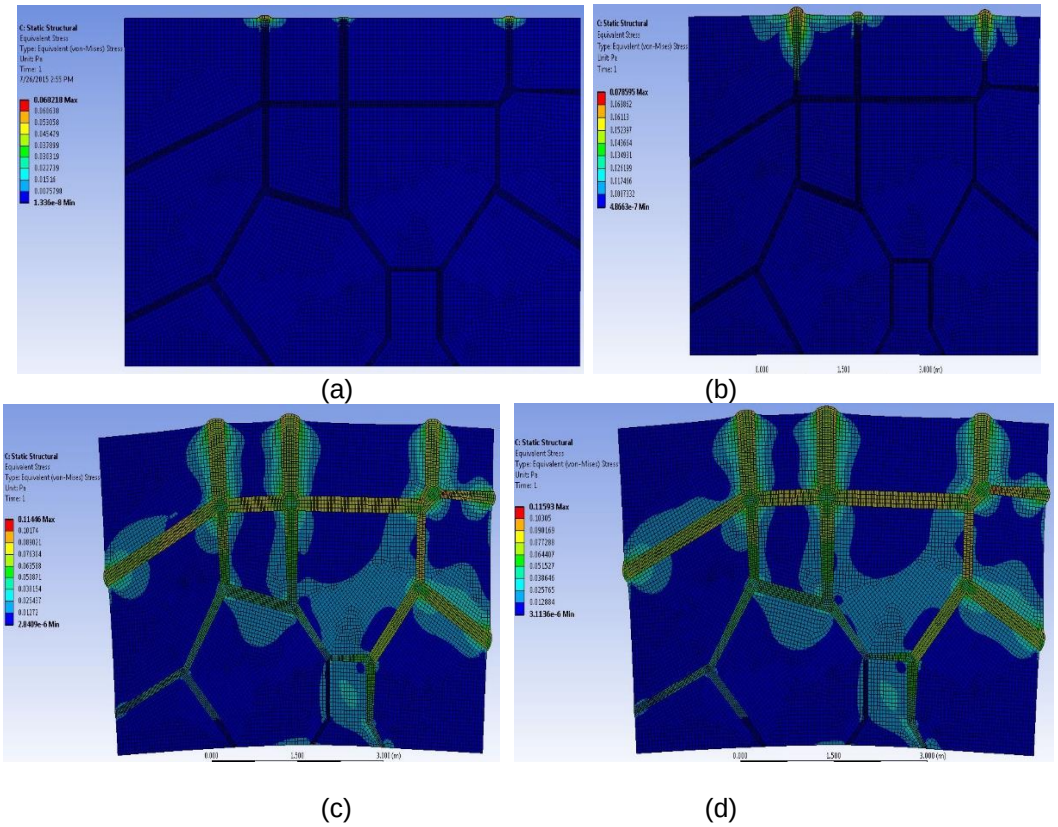

(a) (b)

(c) (d)

Figure 4.16 Equivalent (von – Mises) Stress at (a) t=1.7e-10sec. (b) t= 1.7e-8sec. (c) t= 1.7e-7sec. (d) t= 1.7e-2 sec.

4.2.2.2. Total Plastic Strain

Total plastic strain is important parameter in this study. When hydrogen passes through grain boundary, it produced permanent deformation in grain boundary. This affect original Magnesium nano structure. As grain boundary swells from original shape due to first interaction with hydrogen, this helps coming hydrogen atoms to move faster with in grain boundaries. Hence it is important to have this swelling effect in grain boundaries.

Following figures shows gradual increase in equivalent plastic strain with respect to time. It is important to mention that, most of the total equivalent plastic strain is induced in grain boundary region having higher diffusion coefficient value. Additionally, overall equivalent plastic strain increased with respect to time and never stabilized. To validate this analysis experimental verification is required.

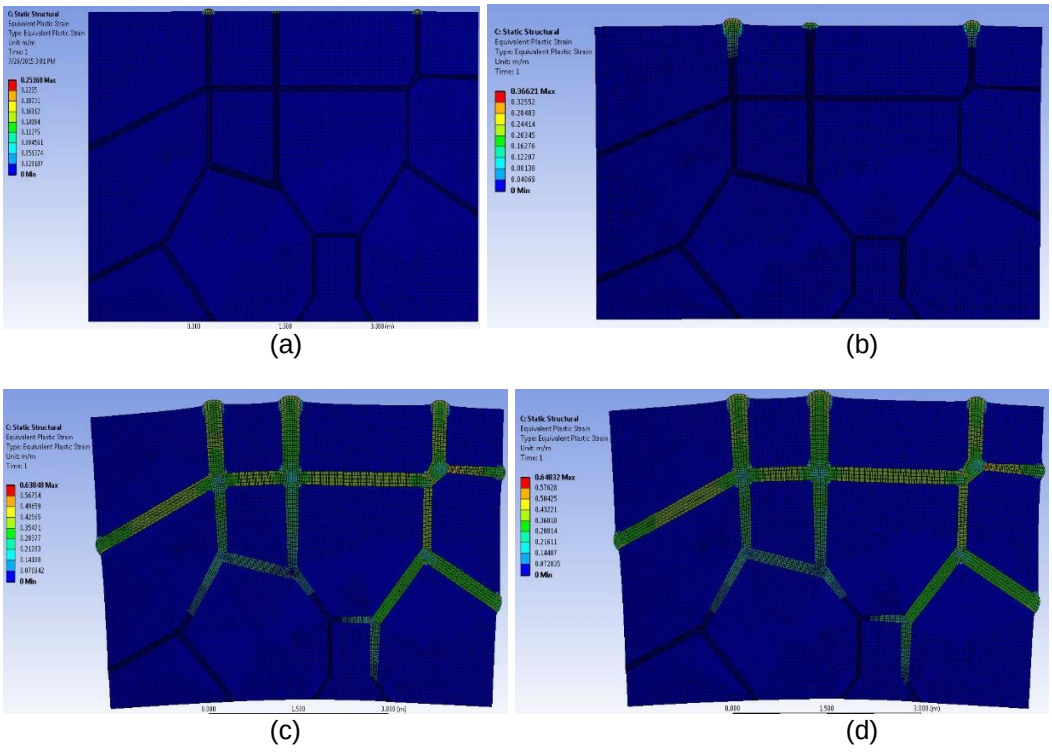

(a) (b)

(c) (d)

Figure 4.17 Equivalent Plastic Strain at (a) t = 1.7e-10sec. (b) t= 1.7e-8sec. (c) t= 1.7e-7sec. (d) t= 1.7e-2 sec.

Chapter 5

CONCLUSION

Solid state hydrogen storage can be an effective way of storing hydrogen as an energy source for mobile applications. The results of the FEM simulation shows that the stress concentration is locate on the grain boundary and bulging of grain boundary causes more hydrogen to pass through it. Different parameters such as diffusion constant, yield strength of grain as well as grain boundary shows different rate of hydrogenation/ dehydrogenation. Twist grain boundary having higher diffusion coefficient produces more deformation within grain boundary which is important for fast charging discharging process. While analyzing overall magnesium nanostructure, it is important to maintained structural integrity between magnesium grains and grain boundaries. Grain boundary having yield strength of 0.05σ'G shows promising results with better charging/discharging process.

For future work, grain boundary could be designed by using cohesive zone technique in ANSYS. Additionally, 3- dimensional modeling could give more precise idea about diffusion process with in grain boundary and chemical stresses induced during hydrogenation/dehydrogenation process.

References

1. Kean Long Lim, Hossein, Kazemian, Zahira Yaakob, Wan Ramli Wan Daud Solid-state Materials and Methods for Hydrogen Storage: A Critical Review. Chem. Eng. Technol. 2010, 33, No. 2, 213–226.
2. Solid State Hydrogen Storage System Design, Solid State Hydrogen Storage Materials and chemistry, Gevin Wlkar (Ed), IBSN 978-1-84569270-4 (book), Y.O.I 2008
3. Magnesium Hydride for Hydrogen Storage, Solid State Hydrogen Storage System Design, Solid State Hydrogen Storage Materials and chemistry, Gevin Wlkar (Ed), IBSN 978-1-84569270-4 (book), Y.O.I 2008
4. P. Jain, Chhagan Lal, Ankur Jain. Hydrogen storage in Mg: A most promising material. Available online: http://www.sciencedirect.com/science/article/pii/S0360319909013615
5. http://upload.wikimedia.org/wikipedia/commons/a/a0/Magnesium-hydride-unitcell 3D-balls.png.
6. M. Pozzo, D. Alfe. Hydrogen dissociation and diffusion on transition metal(=Ti, Zr, Fe, Ru, Co, Rh, Ni, Pd, Cu, Ag)-doped Mg(0001) surfaces. International journal of hydrogen energy, 34 (2009) I922-I930.
7. YAO XiangDong, LU Gao Magnesium based materials for hydrogen storage : Recent advances and future prospective. Chinese Science Bulletin, Vol, 53, No 16, pg. 2421-2431, D.O.I. August 2008.(Available online) http://www.sciencedirect.com/science/article/pii/S0925838805018864
8. Finnabogi Oskarsson, William Stier, Hannes Johnsson. Calculation of binding energy and diffusion of hydrogen in pure magnesium metal and magnesium

hydride. D.O.I 12 November 2003 (Available online) http://theochem.org/bragasetur/papers/MgH.pdf

9. Jolibois PCR. Acad Sci 1912;155(5):353. Wiberg E, Goelttzer H, Bauer R. Z Naturforsch B 1951;6(7):394.
10. Bogdanovic B. Magnesium hydride: a homogeneouscatalysed synthesis and its use in hydrogen storage. International Journal Hydrogen Energy 1984;9(11):937.
11. Bo Yang, Yuping He, Yiping Zhao. Concentration-dependent hydrogen diffusion in hydrogenation and dehydrogenation of vanadium-coated magnesium nanoblades (Available online)http://www.sciencedirect.com/science/article/pii/S036031991102163X
12. Zaluski L, Zaluska A, StromOlsen JO. Nanocrystalline metal hydrides. Journal of Alloys and Compounds 1997; 253:70e9.
13. K. L. Lim, Hydrogen Storage on Activated Carbon Fibers and Carbon Nanotubes, Universiti Kebangsaan Malaysia, Bangi, Malaysia 2008. D. C. Elias et al., Science 2009, 323 (5914), 610.
14. Hydrogen as a future energy carrier. (Ed. By Andreas Zuttel, Andres Boegschulte and Louis Schlapbach), ISBN: 978-3-527-30817-0, D.O.I January 2008.
15. Amitava Moitra, Grain size effect on microstructural properties of 3D nanocrystalline magnesium under tensile deformation, A. Moitra / Computational Materials Science 79 (2013) 247–251
16. Andreas Pedersen, Hannes Jo´nsson, Simulations of hydrogen diffusion at grain boundaries in aluminum, ScienceDirect Acta Materialia 57 (2009) 4036–4045
17. Naoki Matsunaga, Morio Hori and Akira Nagashima, Measurement of Mutual Diffusion Coefficients of Gases by the Taylor Method: Measurements on H2.Air, H2.N2, and H2.O2 Systems, *Heat Transfer—Asian Research*, **31** (3), 2002 182

18. Physiology web, http://www.physiologyweb.com/calculators/diffusion_time_calculator.html
19. R. Kumara, L. Nicolab, E. Van der Giessena, Density of grain boundaries and plasticity size effects: A discrete dislocation dynamics study, (Available online: http://www.sciencedirect.com/science/article/pii/S0921509309009915)
20. Ori Yeheskel, Rachman Chaim, Zhijian Shen and Mats Nygren, Elastic moduli of grain boundaries in nanocrystalline MgO ceramics, J. Mater. Res., Vol. 20, No. 3, Mar 2005

Biographical Information

Amey N. Mathakari completed his undergraduate program in 2012 at Pune University, India. After that, he pursued his master degree in University of Texas at Arlington in August 2013 and started working under the guidance of Dr. Bo Yang in December 2013. During master's program, he has completed internship at Superior Tire & Rubber Corp. Warren, PA. During internship he was involved in material testing of polyurethane and rubber sample, design and analysis of prototype loadwheels, tires and casters. His research interests include finite element analysis, stress analysis, structural design, material characterization, solid state hydrogen storage system and lithium-ion battery.